treated with enzyme at 37 °C for 15 min, cells were seeded on poly-L-lysine-coated coverslips at a density of 2×10^6 cells/cm^3. The cells were maintained for 10–14 days in Dulbecco's modified Eagle's medium (Invitrogen, Grand Island, NY, USA) supplemented with 10% precolostrum newborn calf serum (Invitrogen), 10 U/ml penicillin and 10 μg/ml streptomycin. Standard whole-cell voltage-clamp recordings were made from cultured thalamic neurons at room temperature using an Axopatch 200B amplifier (Axon Instruments, Foster City, CA, USA). To selectively record sodium currents, the pipette solution contained: 115 CsCl, 25 NaCl, 2 $MgCl_2$, 1 $CaCl_2$, 11 EGTA and 10 HEPES, pH 7.4 with CsOH. The external bath solution contained the following (in mM): 100 NaCl, 40 tetraethylammonium-Cl, 0.03 $CaCl_2$, 10 HEPES, 10 $MgCl_2$, 10 D-glucose, pH 7.4 with TEA-OH. The patch microelectrodes were made from borosilicate capillary glass and had resistances of 5–10 MΩ for the whole-cell recording. Under voltage-clamp recording conditions, the series resistance was 4–7 MΩ. Leak currents were subtracted by a P/4 pulse protocol except for the experiments on use-dependent block, and the series resistance was compensated by 70–80% in all experiments. The signals filtered at 2 kHz were directly digitized and stored on a personal computer. These sampled measurements were analyzed using the pCLAMP8 program (Axon Instruments). In repeated tests, voltage steps of 20 ms duration were applied every 20 s from a resting potential of −70 mV to a test potential of −20 mV. Availability protocols consisted of a series of prepulses between −100 mV and −20 mV in 10-mV increments lasting 1 s, from a holding potential of −70 mV, followed by a 20-ms depolarization to −20 mV. The normalized curves were fitted using a Boltzmann distribution equation: $I/I_{max} = 1/(1 + \exp((V_m - V_{1/2})/k))$, where I_{max} is the peak sodium current elicited after the most hyperpolarized prepulse, V_m is the preconditioning pulse potential, $V_{1/2}$ is the potential at which inactivation is half-maximal, and k is the slope factor. Unless otherwise noted, statistical analyses were performed using Student's t-test. The opioid analgesics used in the present study were morphine hydrochloride (Daiichi-Sankyo Co., Tokyo, Japan), fentanyl citrate (a kind gift from Hisamitsu Pharmaceutical Co. Inc., Tokyo, Japan) and oxycodone hydrochloride (a kind gift from Shionogi Pharmaceutical Co. Inc., Osaka, Japan). Lidocaine, naloxone, β-endorphin, endomorphin-1, endomorphin-2 and QX-314 were obtained from Sigma–Aldrich (St. Louis, MO, USA).

To determine if morphine, fentanyl and oxycodone could affect voltage-dependent sodium currents, whole-cell sodium currents were recorded in rat cultured thalamic neurons. Each opioid analgesic and the sodium channel blocker lidocaine reduced sodium currents in a concentration-dependent manner in rat cultured thalamic neurons (Fig. 1B). The IC_{50} values for morphine, fentanyl, oxycodone and lidocaine were 1053 μM (920–1206 μM), 153.2 μM (132.7–170.2 μM), 1260 μM (1135–1398 μM) and 350.2 μM (303.0–404.6 μM), respectively. The suppression of sodium currents was observed immediately after bath application of 100 μM morphine, fentanyl and oxycodone, and these inhibitions were reversible on washing (Supplementary Fig. 1). Under these recording conditions, tetrodotoxin blocked all channel currents (data not shown). In acute thalamic slices, sodium currents were suppressed by 100 μM morphine (Supplementary Fig. 2). To determine whether MOR contributes to the reduction of sodium currents by opioid analgesics, we first tested the effects of the opioid receptor antagonist naloxone on the suppression of sodium currents by opioid analgesics in cultured thalamic neurons. Bath application of 10 μM naloxone failed to block the inhibitory effects of 100 μM morphine (16.5 ± 3.3%; morphine + naloxone, 15.5 ± 3.1%, $n = 7$), fentanyl (35.9 ± 0.6%; fentanyl + naloxone, 35.6 ± 4.8%, $n = 3$) and oxycodone (12.6 ± 1.2%; oxycodone + naloxone, 14.9 ± 1.6%, $n = 4$) (Fig. 1C). Furthermore, to confirm the MOR-independent fashion of the fentanyl-induced suppression of sodium currents, we used thalamic neurons obtained from MOR$^{-/-}$ mice. After the bath application of 100 μM fentanyl, sodium currents were clearly suppressed in thalamic neurons with no detectable MORs ($I/I_0 = 0.659 \pm 0.033$, $p < 0.001$, $n = 5$, Fig. 1D). We next tested whether endogenous μ-opioid peptides could affect the sodium currents in rat cultured thalamic neurons. Application of β-endorphin, endomorphin-1 or endomorphin-2 (1, 10 or 100 μM) did not affect the amplitude of sodium current (100 μM; decrease by 4.0 ± 1.5%, 2.7 ± 0.5%, −1.1 ± 2.9%, respectively, Fig. 1E).

A common property of local anesthetics used clinically is that they preferentially affect the channel at a specific stage in its cycle of rest, activation and inactivation, often by delaying recovery from the inactivated state, thereby producing a cumulative reduction of sodium currents called 'use-dependent' block [5]. In the present study, the suppression of sodium currents by 100 μM fentanyl or lidocaine was use-dependent, as demonstrated by a progressive decrease in current during repetitive stimulation from −100 mV to −20 mV at 10 Hz (Fig. 2A and D). After the bath application of 100 μM fentanyl or lidocaine, the ratio of current amplitude was decreased at the first pulse (34.7 ± 2.1%, $n = 5$, or 13.6 ± 6.6%, $n = 4$, respectively), and at the 10th pulse (55.2 ± 1.9% or 31.0 ± 4.6%, respectively), compared with before drugs (Fig. 2B and E). A further analysis of the pulse-by-pulse decrease revealed that the suppression of sodium current by fentanyl or lidocaine was use-dependent (first pulse versus 10th pulse; 31.5 ± 1.6% or 29.0 ± 7.9%, respectively, Fig. 2C and F).

Local anesthetics can produce hyperpolarizing shifts in steady-state inactivation by binding to a receptor site on the ion channel [1,7]. In the present study, the application of 100 μM morphine (−4.8 ± 1.1 mV, $n = 7$), fentanyl (−8.6 ± 0.9 mV, $n = 7$), oxycodone (−3.6 ± 0.4 mV, $n = 4$) and lidocaine (−9.3 ± 0.6 mV, $n = 3$) caused hyperpolarizing shifts in $V_{1/2}$ of steady-state inactivation (Fig. 2G–J).

Most local anesthetics used clinically are relatively hydrophobic molecules that gain access to their blocking site on the sodium channel by diffusing into or through the cell membrane [7]. To determine the apparent sidedness of drug action, we measured the sodium currents elicited by a depolarizing step pulse (from −70 mV to −20 mV, 20 ms) in cells filled with each opioid analgesic or lidocaine. QX-314, a positively charged derivative of lidocaine, has no effect on neuronal sodium channels when applied extracellularly, but blocks sodium channels when applied intracellularly [2,6,17]. Consistent with this finding, QX-314 (10 mM) totally suppressed sodium current in our experiments (Fig. 3A and B). The addition of oxycodone, fentanyl or lidocaine at 10 mM to the recording pipette had no effect on sodium currents compared with a control pipette solution (peak amplitude = −3099.4 ± 140.4 pA with oxycodone, $n = 4$, −2850.5 ± 572.8 pA with fentanyl, $n = 5$, −2522.4 ± 569.6 pA with lidocaine, $n = 4$, Fig. 3A and B), whereas the sodium current was almost totally abolished by bath application of these drugs at the same concentration (Fig. 1B). On the other hand, the addition of 10 mM morphine to the recording pipette significantly reduced sodium currents (peak amplitude = −897.7 ± 119.0 pA, $p < 0.001$, $n = 6$, Fig. 3A and B). We also asked whether the intracellular application of fentanyl or lidocaine could affect the suppression of sodium currents caused by the extracellular application of fentanyl or lidocaine. In the presence of intracellular fentanyl or lidocaine at 10 mM, extracellular application of 100 μM fentanyl or lidocaine caused current suppression (39.7 ± 0.2% or 26.0 ± 0.2%, respectively, Fig. 3C). Furthermore, this was observed at approximately the same level as in the absence of intracellular fentanyl or lidocaine (37.0 ± 2.0% or 22.9 ± 1.8%, respectively, Fig. 3C).

It has been well established that opioid analgesics inhibit cAMP formation, close voltage-sensitive Ca^{2+} channels and open K^+ channels though MOR, which leads to cell hyperpolarization and exerts an inhibitory effect [3,4,14]. In this study, we used whole-cell voltage-clamp recording and found that, as with lidocaine, extra-

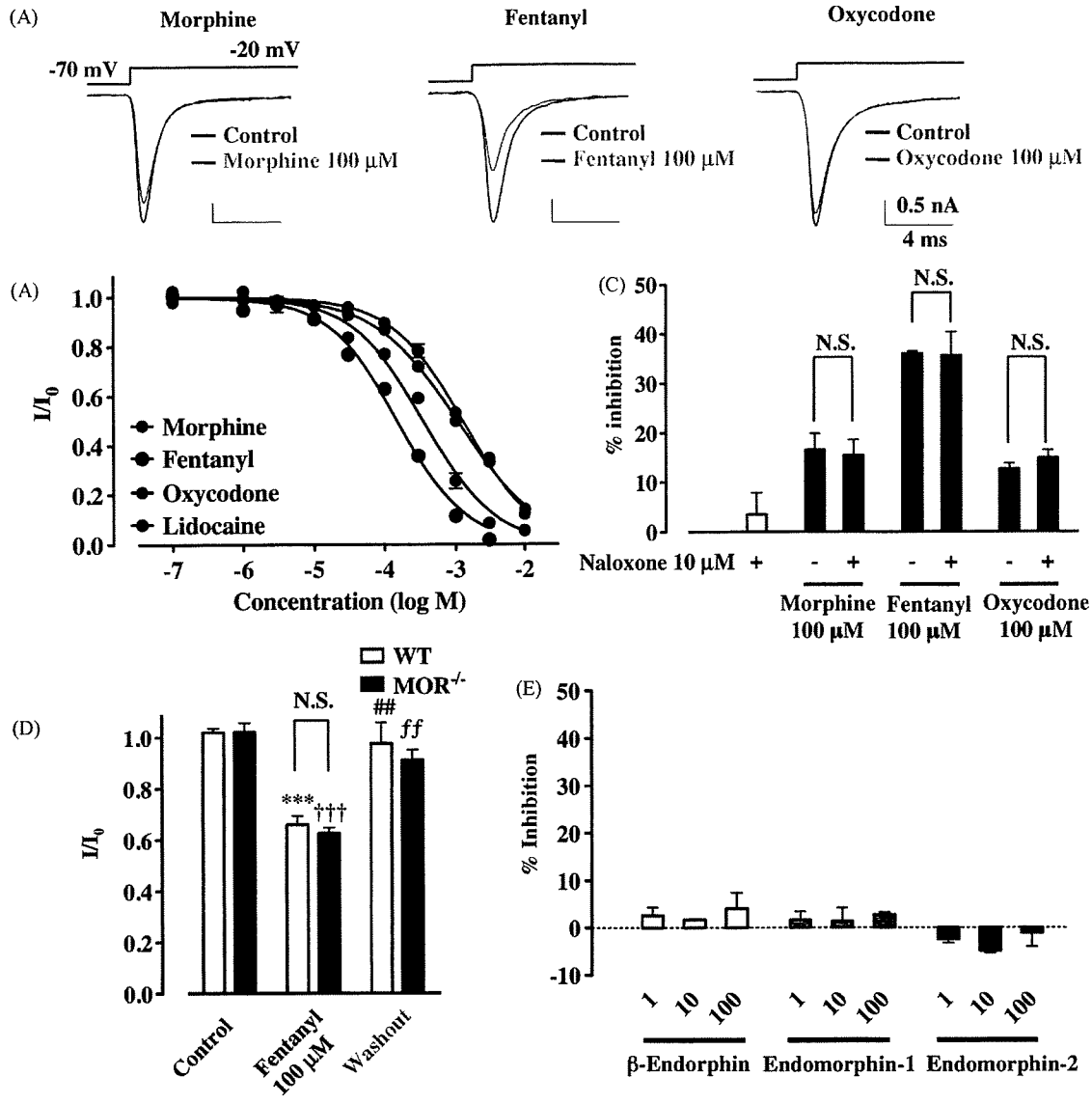

Fig. 1. Suppression of sodium currents by opioid analgesics in rat thalamic neuron through non-opioidergic mechanisms. Voltage steps were applied from a holding potential of −70 mV to a test potential of −20 mV. (A) Representative current traces obtained in the presence or absence of 100 μM morphine, fentanyl or oxycodone. (B) Concentration-dependent inhibition of the sodium currents by morphine, fentanyl, oxycodone and lidocaine in rat cultured thalamic neurons. Each symbol represents the mean value of normalized peak currents in the presence of drug (I/I_0, mean ± S.E.M.), derived from 3 to 8 independent experiments for each concentration tested. (C) No effects of the opioid receptor antagonist naloxone (10 μM) on suppression of sodium currents by the bath application of 100 μM morphine, fentanyl or oxycodone. (D) No involvement of MORs in fentanyl-induced suppression of sodium currents in thalamic neurons using $MOR^{-/-}$ mice. Each column represents the normalized peak current amplitudes (I/I_0, mean ± S.E.M., $n = 5$). $^{***}p < 0.001$ control (WT) vs. fentanyl (WT), $^{\#\#}p < 0.01$ fentanyl (WT) vs. washout (WT), $^{\dagger\dagger\dagger}p < 0.001$ control ($MOR^{-/-}$) vs. fentanyl ($MOR^{-/-}$), $^{ff}p < 0.01$ fentanyl ($MOR^{-/-}$) vs. washout ($MOR^{-/-}$). (E) Effects of endogenous μ-opioid peptides on voltage-gated sodium channels in rat cultured thalamic neurons. No significant changes in sodium currents were observed with the bath application of 1–100 μM β-endorphin ($n = 5$–7), endomorphin-1 ($n = 3$) or endomorphin-2 ($n = 3$–8). Each column represents the mean value of the %inhibition of the peak amplitude of the sodium currents in the presence of drug (mean ± S.E.M.).

cellular application of morphine, fentanyl or oxycodone produced a concentration-dependent suppression of sodium currents, which was not influenced by the opioid receptor antagonist naloxone. In agreement with these findings, the effect of fentanyl on sodium current suppression was clearly shown in thalamic neurons obtained from $MOR^{-/-}$ mice. Moreover, endogenous μ-opioid peptides did not affect the amplitude of sodium currents. These findings clearly indicate that morphine, fentanyl and oxycodone suppress thalamic sodium currents through non-opioidergic mechanisms.

We also found that, among these opioids, the inhibitory potency of the extracellular application of fentanyl was much stronger than those of the other two opioids, to the same degree as lidocaine. Although further study is required, the similarity of the chemical structures of fentanyl and lidocaine may help to explain the similarity of their potencies, as well as the difference in the sodium channel-blocking effects of fentanyl, morphine or oxycodone. There is a broad consensus that most local anesthetics used clinically gain access to their blocking site on the sodium channel by diffusing into or through the cell membrane [7]. In addition, the site at which local anesthetics act, at least in their charged form, is accessible only from the inner surface of the membrane [10]. Lidocaine, morphine, oxycodone and fentanyl have pK_a values of 7.8, 7.9, 8.5 and 8.4, respectively, which means that more than 80% of the drug is ionized at physiological pH. Even though large amounts of lidocaine, fentanyl and oxycodone are ionized at experimental pH, the present data clearly show that the internal application of fentanyl, oxycodone or lidocaine failed to suppress sodium currents, whereas external application of the same drugs suppressed sodium currents

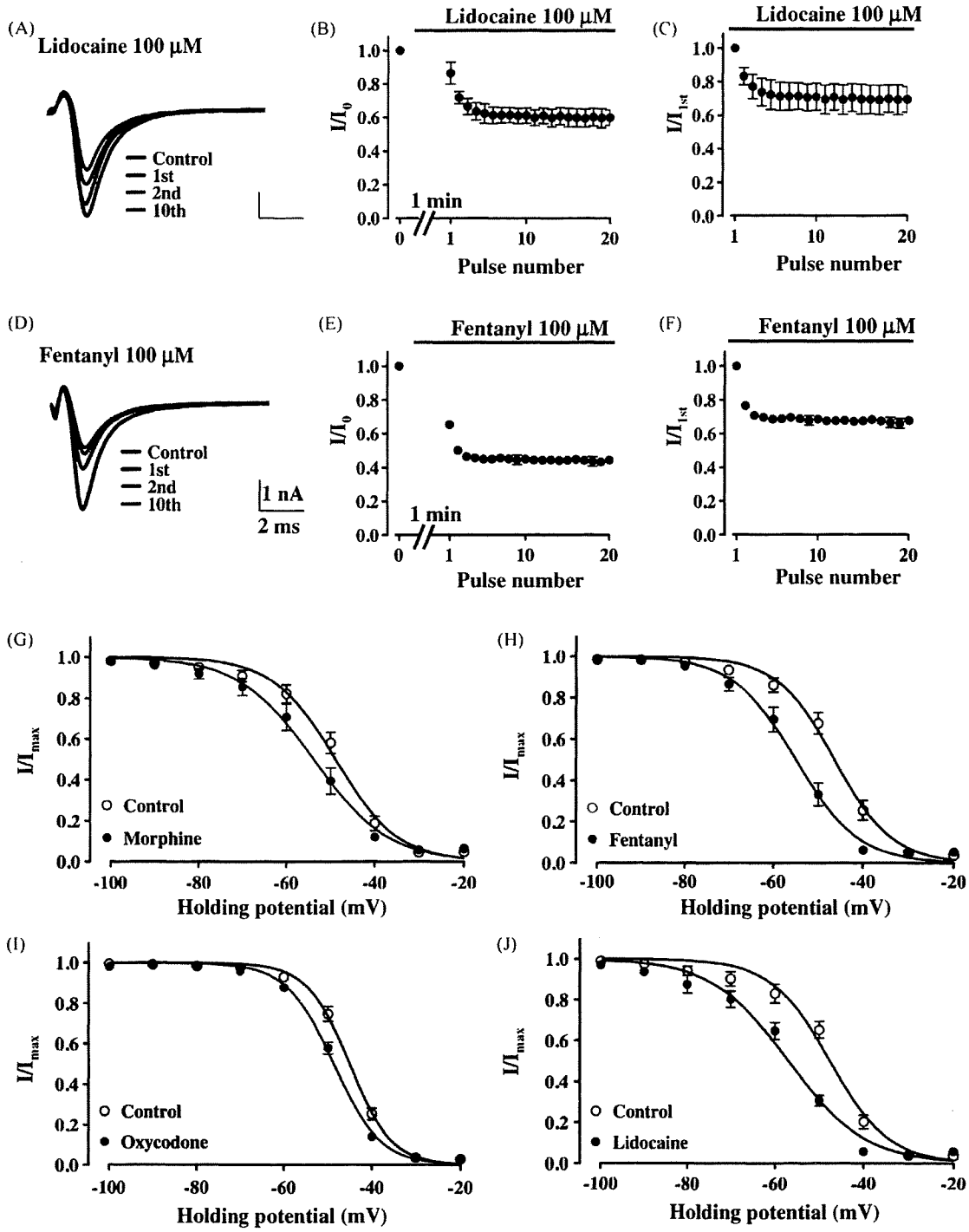

Fig. 2. A common feature of the effects of opioid analgesics and local anesthetics on sodium current suppression. (A–F) Use-dependent block of sodium currents by lidocaine and fentanyl. Use-dependent block was examined at 10 Hz with 30 20-ms test pulses to −20 mV from a holding potential of −100 mV. Repeated test potentials were given 1 min after the bath application of 100 μM lidocaine or fentanyl. (A and D) Representative traces show currents elicited by the pre-drug (Control) and first (1st), second (2nd) or 10th pulses after the bath application of lidocaine or fentanyl. (B, C, E, F) Time-course changes in use-dependent block. Peak current amplitudes were normalized to the control peak current amplitude (I/I_0, mean ± S.E.M., B and E) or to the initial peak current amplitude in the presence of drug (I/I_{1st}, mean ± S.E.M., C and F) and plotted against the pulse number. (G–J) Voltage-dependence of inactivation for the sodium current in rat cultured thalamic neurons. The voltage-dependence of channel inactivation in the absence (Control) and presence of 100 μM morphine (G), fentanyl (H), oxycodone (I) or lidocaine (J) was estimated by measuring the peak amplitude of the sodium current during a test potential (−20 mV) from a variable holding potential. The current at each membrane potential was divided by the electrochemical driving force for sodium ions and normalized to the maximum sodium current (I_{max}).

with different potencies. Furthermore, in the presence of intracellular fentanyl or lidocaine, extracellular application of fentanyl or lidocaine, respectively, caused current suppression to approximately the same level as that in the absence of intracellular fentanyl or lidocaine. This phenomenon induced by lidocaine is consistent with a recent report that external, but not internal, application of the sodium channel blocker flecainide promotes use-dependent block of heart sodium channels [8]. Thus, the present data strongly suggest that either fentanyl- or lidocaine-induced sodium current suppression may occur when drugs are present extracellularly. In

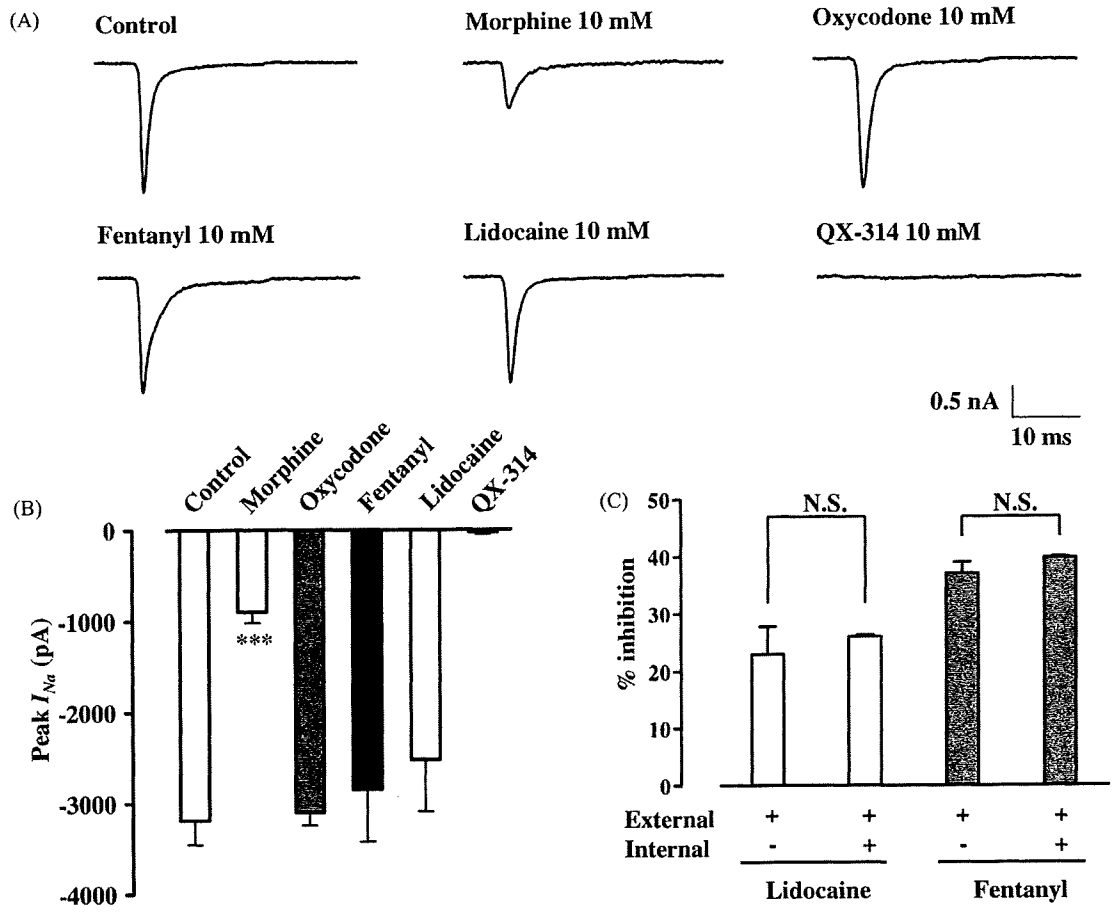

Fig. 3. The effect of intracellular application of opioid analgesics in whole-cell configurations. (A) Representative traces show the currents in a control pipette solution and in the presence of intracellular morphine (10 mM), oxycodone (10 mM), fentanyl (10 mM), lidocaine (10 mM) and the lidocaine derivative QX-314 (10 mM). Currents were elicited by 20-ms depolarizing steps from a holding potential of −70 mV to a test potential of −20 mV. Pulses were applied until steady-state sodium currents were achieved. (B) Bar graphs summarize steady-state sodium currents with the internal application of morphine, oxycodone, fentanyl, lidocaine and QX-314. Each column represents the mean value of the peak currents with S.E.M. $^{***}p < 0.001$ vs. control. (C) Test of sidedness of fentanyl block using whole-cell recordings. Suppression of sodium currents by the extracellular application of 100 μM lidocaine or fentanyl was measured in the absence or presence of intracellular lidocaine (10 mM) or fentanyl (10 mM). Each column represents the mean value of the %inhibition of the peak amplitude of the sodium currents in the presence of drugs (mean ± S.E.M.).

contrast, morphine caused a significant suppression of sodium currents when applied either internally or externally, but with different potencies. These findings suggest that, like lidocaine, either fentanyl or oxycodone may have a blocking effect on sodium currents by acting through the extracellular pathway, whereas morphine may act through both the extracellular and intracellular pathway.

Use-dependent block, where the inhibitory effect on channels by a drug cumulatively increases with repetitive stimulation at high frequency, which mostly indicates that the drug can block the channel current when the channel is activated (open), is the hallmark for local anesthetics. In the present study, depending on the pulse number, both lidocaine and fentanyl progressively decreased the peak amplitude of sodium currents at a holding potential of −100 mV, indicating that fentanyl effectively blocks the sodium channel current when the channel gate is open. We also found that fentanyl, but not lidocaine, caused the tonic suppression of sodium currents with no depolarizing stimulation at a holding potential of −100 mV, and that almost all thalamic sodium channels were maintained with a resting state. These findings suggest that the inhibition of sodium channels by fentanyl may result from its multiple effects on sodium channels in both the resting and activated (channel open) states.

It has been reported that a local anesthetic binds more tightly to and stabilizes the inactivated state of the sodium channel [1,5,7]. Consistent with these observations with local anesthetics, we demonstrated that lidocaine showed hyperpolarizing shifts in the steady-state inactivation of voltage-gated sodium channels. Under the present conditions, we found that the extracellular application of these three opioids gave the same performance as with exposure to lidocaine. The present data suggest that, like lidocaine, morphine, fentanyl and oxycodone suppress sodium currents by facilitating inactivation of a thalamic sodium channel at a normal resting membrane potential when these three opioids are applied extracellularly.

In conclusion, we have shown that opioid analgesics in thalamic neurons may promote the inhibition of neuronal activity by blocking voltage-gated sodium channels without MOR activation. Furthermore, our data suggest that three MOR agonists exhibit different blocking potencies toward sodium channels with distinct mechanisms. In future studies, it might be worthwhile to ascertain whether these opioid analgesics directly access their binding domains on voltage-gated sodium channels and how to facilitate their blocking effects.

Appendix A. Supplementary data

Supplementary data associated with this article can be found, in the online version, at doi:10.1016/j.neulet.2009.01.066.

References

[1] B.P. Bean, C.J. Cohen, R.W. Tsien, Lidocaine block of cardiac sodium channels, J. Gen. Physiol. 81 (1983) 613–642.
[2] M.D. Cahalan, W. Almers, Interactions between quaternary lidocaine, the sodium channel gates, and tetrodotoxin, Biophys. J. 27 (1979) 39–55.
[3] S.R. Childers, Opioid receptor-coupled second messenger systems, Life Sci. 48 (1991) 1991–2003.
[4] M.J. Christie, R.A. North, Agonists at mu-opioid, M2-muscarinic and GABAB-receptors increase the same potassium conductance in rat lateral parabrachial neurones, Br. J. Pharmacol. 95 (1988) 896–902.
[5] K.R. Courtney, Mechanism of frequency-dependent inhibition of sodium currents in frog myelinated nerve by the lidocaine derivative GEA, J. Pharmacol. Exp. Ther. 195 (1975) 225–236.
[6] D.T. Frazier, T. Narahashi, M. Yamada, The site of action and active form of local anesthetics. II. Experiments with quaternary compounds, J. Pharmacol. Exp. Ther. 171 (1970) 45–51.
[7] B. Hille, Local anesthetics: hydrophilic and hydrophobic pathways for the drug-receptor reaction, J. Gen. Physiol. 69 (1977) 497–515.
[8] H. Liu, J. Atkins, R.S. Kass, Common molecular determinants of flecainide and lidocaine block of heart Na+ channels: evidence from experiments with neutral and quaternary flecainide analogues, J. Gen. Physiol. 121 (2003) 199–214.
[9] H. Mizoguchi, H.E. Wu, M. Narita, I. Sora, S.F. Hall, G.R. Uhl, H.H. Loh, H. Nagase, L.F. Tseng, Lack of mu-opioid receptor-mediated G-protein activation in the spinal cord of mice lacking Exon 1 or Exons 2 and 3 of the MOR-1 gene, J. Pharmacol. Sci. 93 (2003) 423–429.
[10] T. Narahashi, D.T. Frazier, Site of action and active form of local anesthetics, Neurosci. Res. 4 (1971) 65–99.
[11] M. Narita, K. Hashimoto, T. Amano, M. Narita, K. Niikura, A. Nakamura, T. Suzuki, Post-synaptic action of morphine on glutamatergic neuronal transmission related to the descending antinociceptive pathway in the rat thalamus, J. Neurochem. 104 (2008) 469–478.
[12] M. Narita, A. Nakamura, M. Ozaki, S. Imai, K. Miyoshi, M. Suzuki, T. Suzuki, Comparative pharmacological profiles of morphine and oxycodone under a neuropathic pain-like state in mice: evidence for less sensitivity to morphine, Neuropsychopharmacology 33 (2008) 1097–1112.
[13] M. Narita, M. Ohsawa, H. Mizoguchi, T. Aoki, T. Suzuki, L.F. Tseng, Role of the phosphatidylinositol-specific phospholipase C pathway in delta-opioid receptor-mediated antinociception in the mouse spinal cord, Neuroscience 99 (2000) 327–331.
[14] H. Rhim, R.J. Miller, Opioid receptors modulate diverse types of calcium channels in the nucleus tractus solitarius of the rat, J. Neurosci. 14 (1994) 7608–7615.
[15] D. Smart, G. Smith, D.G. Lambert, Mu-opioids activate phospholipase C in SH-SY5Y human neuroblastoma cells via calcium-channel opening, Biochem. J. 305 (1995) 577–581.
[16] I. Sora, N. Takahashi, M. Funada, H. Ujike, R.S. Revay, D.M. Donovan, L.L. Miner, G.R. Uhl, Opiate receptor knockout mice define mu receptor roles in endogenous nociceptive responses and morphine-induced analgesia, Proc. Natl. Acad. Sci. U.S.A. 94 (1997) 1544–1549.
[17] G.R. Strichartz, The inhibition of sodium currents in myelinated nerve by quaternary derivatives of lidocaine, J. Gen. Physiol. 62 (1973) 37–57.

Neuroscience 164 (2009) 1252–1262

SUBDIAPHRAGMATIC VAGOTOMY PROMOTES NOCICEPTIVE SENSITIVITY OF DEEP TISSUE IN RATS

S. FURUTA,[a] T. SHIMIZU,[a] M. NARITA,[a]
K. MATSUMOTO,[a,b] N. KUZUMAKI,[a] S. HORIE,[b]
T. SUZUKI[a]* AND M. NARITA[a]*

[a]*Department of Toxicology, Hoshi University School of Pharmacy and Pharmaceutical Sciences, 2-4-41 Ebara, Shinagawa-ku, Tokyo, 142–8501, Japan*

[b]*Laboratory of Pharmacology, Faculty of Pharmaceutical Sciences, Josai International University, 1 Gumyo, Togane, Chiba 283–8555, Japan*

Abstract—To verify whether vagal dysfunction is associated with chronic pain, we evaluated the effects of subdiaphragmatic vagotomy (vgx) on the sensitivity toward noxious stimuli in rats. Vgx rats showed sustained hyperalgesia in the gastrocnemius muscle without tissue damage (no increase in vgx-induced plasma creatine phosphokinase or lactose dehydrogenase levels) accompanied by hypersensitivity to colonic distension. We found a dramatic increase in the levels of metabotropic glutamate receptor 5, protein kinase C (PKC) γ and phosphorylated-PKCγ within the spinal cord dorsal horn in vgx rats, which suggests that vgx may evoke sensory nerve plasticity. Morphine produced a dose-dependent increase in the withdrawal threshold in both vgx and sham-operated rats, but the effect of a lower dose in vgx rats was weaker than that in sham-operated rats. Muscle hyperalgesia in vgx rats was also attenuated by gabapentin and amitriptyline, but was not affected by diclofenac, dexamethasone or diazepam. These findings indicate that subdiaphragmatic vagal dysfunction caused chronic muscle hyperalgesia accompanied by visceral pain and both gabapentin and amitriptyline were effective for subdiaphragmatic vagotomy-induced pain, which are partially similar to fibromyalgia syndrome. Furthermore, this chronic muscle pain may result from nociceptive neuroplasticity of the spinal cord dorsal horn.

Key words: chronic pain, muscle hyperalgesia, vagotomy, subdiaphragmatic vagus nerve, fibromyalgia syndrome, rat.

The change of the activity in the vagus nerve, especially the subdiaphragmatic vagus nerve, affects nociceptive responses. In animal experiments, electrical stimulation of the subdiaphragmatic vagus nerve produced inhibition of the tail-flick reflex in rats (Ren et al., 1988; Randich and Gebhart, 1992). In addition, vagal stomach afferent activation had an inhibitory effect on somatic pain perception in humans (Sedan et al., 2005). On the other hand, Holtmann et al. (1998) reported lower thresholds for the perception of pain in patients who had previously undergone vagotomy in the course of a Billroth I gastrectomy, compared to those in healthy controls. It has been also reported that subdiaphragmatic vagotomy is associated with cutaneous mechanical hyperalgesia (Khasar et al., 1998a,b) and visceral hypersensitivity (Gschossmann et al., 2002; Chen et al., 2008) in rats. However, there is no report to investigate whether subdiaphragmatic vagotomy decreases the pain threshold of deep tissue, including muscle. Furthermore, it is unknown whether subdiaphragmatic vagotomy induces neuroplasticity in the spinal cord dorsal horn and which types of drugs are effective on subdiaphragmatic vagotomy-induced pain. The aim of the present study was to characterize subdiaphragmatic vagal dysfunction-induced pain using the subdiaphragmatic vagotomized rats.

EXPERIMENTAL PROCEDURES

The present study was conducted in accordance with the Guiding Principles for the Care and Use of Laboratory Animals, Hoshi University, as adopted by the Committee on Animal Research of Hoshi University. Every effort was made to minimize the numbers and any suffering of animals used in the following experiments.

Animals

The experiments were performed on male 8–9 week-old Sprague–Dawley rats (weighting approximately 300 g) purchased from Nippon SLC (Shizuoka, Japan) for the colorectal balloon distension test and mechanical hyperalgesia test, and Tokyo Laboratory Animals Science (Tokyo, Japan) for all the other experiments. The animals were normally fed standard laboratory food and water and housed in temperature (23±1 °C) controlled rooms under a 12 h/12 h light/dark cycle.

Drugs

The drugs used in the present study were morphine hydrochloride (Daiichi-Sankyo, Tokyo, Japan), gabapentin (Tocris, Ellisville, MO, USA), diazepam (Wako Pure Chemical Industries, Osaka, Japan), dexamethasone (MP Biomedicals, Vannes, France), 1% xylocaine (Astrazeneca, Osaka, Japan), and amitriptyline and diclofenac sodium (Sigma Chemical Co, St. Louis, MO, USA). Diazepam was suspended in 9% Tween 80-saline solution, and the other drugs, except xylocaine, were dissolved in freshly prepared 0.9% sterile physiological saline. These drugs were s.c. or i.v. administered in a volume of 1 ml/kg. Intracutaneous and i.m. 1% xylocaine was administered in volumes of 0.05 ml/site and 0.1 ml/site, respectively.

*Corresponding authors. Tel: +81-3-5498-5628; fax: +81-3-5498-5628.
E-mail address: narita@hoshi.ac.jp (M. Narita); suzuki@hoshi.ac.jp (T. Suzuki).

Abbreviations: AUC, area under curve; CNS, central nervous system; CPK, creatine phosphokinase; CRD, colorectal distension; DBP, diastolic blood pressure; EMG, electromyographic; FMS, fibromyalgia syndrome; HR, heart rate; IR, immunoreactivity; L5, lumbar 5; LDH, lactose dehydrogenase; MBP, mean blood pressure; mGluR5, metabotropic glutamate receptor 5; MPE, maximum possible effect; NGS, normal goat serum; NPY, neuropeptide Y; PBS, phosphate buffered saline; PKC, protein kinase C; RVM, rostral ventral medulla; SBP, systolic blood pressure.

0306-4522/09 $ - see front matter
doi:10.1016/j.neuroscience.2009.09.021

Subdiaphragmatic vagotomy

The animals were anesthetized i.p. with 50 mg/kg pentobarbital sodium (Nakarai chemicals, Tokyo, Japan). After an upper midline laparotomy was performed, the stomach and lower esophagus were exposed at the subdiaphragmatic level. Anterior and posterior vagus trunks were dissected from the esophagus and were cut into at least 0.5-cm sections bilaterally. In addition, so that we could transect small vagus nerve branches, the left gastric artery was isolated, and all connective tissues surrounding the esophagus were removed. To prevent excessive occlusion of the pyloric sphincter after subdiaphragmatic vagotomy, surgical pyloroplasty was performed as follows. An incision was made parallel to the axis of the pylorus, through the pyloric sphincter, and then the pylorus wall was reconstructed by 7-0 silk sutures perpendicular to the pylorus axis. The stomach was returned to its normal position. After thorough i.p. irrigation with warm saline, penicillin G (10,000 U/body) (Meiji Seika kaisha, Tokyo, Japan) was administered i.p.. Muscle and skin layers were closed separately using nylon suture. Sham-operated animals were prepared, subjected only to pyloroplasty. To confirm the loss of body weight in subdiaphragmatic vagotomized rats, which showed that subdiaphragmatic vagotomy was successful (Opsahl and Powley, 1977; Kraly et al., 1986), body weights were measured through the experiments.

Assessment of pain-related behavior

To avoid potential bias, the person performing the behavioral testing, a well-trained tester, was blinded as to the experimental group in this study.

Pressure stimulus to the calf. The pressure-induced paw-withdrawal threshold was measured with a Randall-Selitto apparatus (Muromachi Kikai, Tokyo, Japan) by the modified method of Randall and Selitto (1957) to assess the pain threshold of deep tissue as reported by Fujii et al. (2008). The rate of force and the cut-off value were set at 10 mmHg/s and 150 mmHg, respectively. Before taking measurement, rats were habituated to the testing procedure for 2 days. The upper body of the animal was wrapped in a towel for light restraint. The probe, with a tip diameter of 9 mm, was applied to the calves with an interval of 2 min between measurements. The withdrawal threshold in response to pressure stimulation was determined as the average of the values of three of five trials (excluding the maximum and minimum values). In a preliminary study, we did not find any differences in the withdrawal threshold between the right and left calves. Therefore, the mean value of the withdrawal threshold of both calves was used in this study.

The effects of various analgesic drugs (xylocaine, morphine, diclofenac, dexamethasone, gabapentin, amitriptyline, diazepam) were evaluated from 10 to 26 days after the operation because this was a stable period of a lower withdrawal threshold. The doses of all drugs were determined based on the results of a pilot study and by referring to previous reports (Tonussi and Ferreira, 1994; Buritova et al., 1996; Esser and Sawynok, 1999; Raghavendra et al., 2002; Urban et al., 2005; Beyreuther et al., 2006; Munro et al., 2008). To compare the effects of morphine between sham-operated and subdiaphragmatic vagotomy (vgx) rats, the percent maximum possible effect (%MPE) was calculated as follows: (post-administration value−pre-administration value)/(150 mmHg (cut-off value)−pre-administration value). To decrease the number of animals used in this study, a crossover paradigm was used. Most of the rats were used for one vehicle and one drug treatment with 1–4 days between periods. We also created a washout period of from 3 to 7 days between the experiments to investigate the effect of another drug in the same animal.

Mechanical stimulus to the skin of the calf. The mechanical nociceptive response of the same region of skin, where applying a pressure stimulus to the calf, was measured using a modification of the pin-prick method described by Tal and Bennett (1994). Briefly, after body hair was shaved, the mechanical nociceptive response was assessed by applying a brief pricking stimulation with a 26 G needle, the tip of which had been cut to prevent penetration of the skin, under strictly restrained conditions. The number of pain-related behaviors defined as vocalizations was counted during application of the needle five times to the skin. To investigate the effect of the intracutaneous administration of 1% xylocaine, the number of vocalizations was again counted at 0, 5, 10, 15 and 30 min after injection. The experiment was performed from 18 to 23 days after operation.

Colorectal balloon distension (CRD). Contraction of the abdominal wall in response to a noxious visceral stimulus in rats was quantified through electromyographic (EMG) recordings as described by Ness and Gebhart (1988). For abdominal EMG recordings, bipolar electrodes were implanted into the external oblique muscle under anesthetized with isoflurane. The EMG electrodes were then tunneled s.c. and externalized at the nape of the neck for future access. After surgery, the rats were allowed to recover for 3 days prior to testing. Pressure-controlled CRD were performed with an air inflated distension balloon catheter connected to an electronic distension device (Distender Series II, G&J Electronics, Toronto, Canada). Before starting the CRD, all rats were sufficiently habituated to the acrylic holder for more than 15 min. A polyethylene balloon (1.5 cm diameter) was inserted intra-anally into the colon such that its caudal end was 5 cm proximal to the anus, and was kept in place by taping the catheter to the base of the tail. The EMG activity was recorded for 5 min prior to colonic distension as baseline, and for 5 min during CRD to 80 mmHg and calculated the area under curve (AUC) of EMG amplitude at each period.

Thermal stimulus to the planter surface of the hind paw. The latency of paw withdrawal evoked by thermal stimuli was measured with a thermal stimulus apparatus (Ugobasile, Varese, Italy). The intensity of the thermal stimulus was adjusted to achieve an average baseline paw-withdrawal latency of approximately 8–10 s in sham-operated rats. The upper body of the animal was wrapped in a towel for light restraint. Each hind paw was measured alternatively at intervals of more than 5 min. The latency of paw withdrawal in response to a thermal stimulus was determined as the average of two measurements per paw. In a preliminary study, we did not find any difference in the withdrawal latency between the right and left hind paws, so the mean value of the withdrawal latency of the right and left paws was used in this study.

Mechanical stimulus to the planter surface of the hind paw. Mechanical paw withdrawal threshold was measured by a Dynamic Plantar Aesthesiometer (Ugo Basile, Varese, Italy). Rats were allowed to move freely in acryl box on the metal mesh surface. Rats were sufficiently adapted to the testing environment before measurements, the mechanical stimulus was delivered to the plantar surface of the hind paw from below the floor of the test chamber by an automated testing device. A steel rod was pushed against the hind paw with ascending force (50 g in 20 s). Each hind paw was measured alternatively at intervals of more than 5 min. The threshold of paw withdrawal in response to a mechanical stimulus was determined as the average of three measurements per paw. The threshold was taken as the force applied to elicit a reflex removal of the hind paw. In a preliminary study, we did not find any differences in the withdrawal threshold between the right and left hind paws, so that the mean value of the withdrawal threshold of the right and left paws could be used in this study.

Immunohistochemistry. Rats were perfusion-fixed with 4% paraformaldehyde (pH 7.4) under anesthesia by isoflurane inhalation. After perfusion, the lumbar five spinal cord segments were quickly removed and post-fixed in 4% paraformaldehyde for 2 h. The lumbar five spinal cord segments were then permeated with

20% sucrose in 0.1 M phosphate buffered saline (PBS) for 1 day and 30% sucrose in 0.1 M PBS for 2 days with agitation. Next, these segments were frozen in embedding compound (Sakura Fintechnical, Tokyo, Japan) on isopentane using liquid nitrogen, and stored at −30 °C until use. Frozen the lumbar five spinal cord segments were cut with a freezing cryostat (Leica CM 1510, Leica Microsystems AG, Wetzlar, Germany) at a thickness of 10 μm and thaw-mounted on poly-L-lysine-coated glass slides. The spinal cord sections were blocked in 10% normal goat serum (NGS) in 0.01 M PBS for 1 h at room temperature. Each primary antibody was diluted in 0.01 M PBS containing 10% NGS (1:5000 metabotropic glutamate receptor 5 (mGluR5)) (Upstate USA, VA, USA), 1:3000 protein kinase C (PKC)γ (Santa Cruz, CA, USA), 1:100 phosphorylated-PKCγ (Cell Signaling, MA, USA), and incubated for two nights at 4 °C. The unbound antibody was then rinsed off and incubated with secondary antibodies conjugated with AlexaTM fluo488 (1:1500; for mGluR5, 1:1500; for PKCγ, 1:1000; for phosphorylated-PKCγ) diluted in 0.01 M PBS containing 10% NGS for 2 h at room temperature. The slides were coverslipped with PermaFluor Aqueous mounting medium (Immunon, Pittsburgh, PA, USA). The fluorescence of immunolabeling was detected using a light microscope (Olympus AX-70; Olympus, Tokyo, Japan). Digitized images of the superficial laminae of spinal cord dorsal horn sections were captured at a resolution of 1316×1035 pixels with a digital camera (Polaroid PDMCII/OL; Olympus). The density of mGluR5, PKCγ and phosphorylated-PKCγ labeling was measured with a computer-assisted image-analysis system (NIH Image, developed at the National Institutes of Health, available at http://rsb.info.nih.gov/nih.image). The upper and lower threshold density ranges were adjusted to encompass and match the immunoreactivity; this provided an image with immunoreactive material appearing as black pixels and non-immunoreactive material as white pixels. A standardized rectangle was positioned over the superficial laminae of the dorsal horn of the spinal cord area from sham-operated rats. The area and density of pixels within the threshold value representing immunoreactivity were calculated, and the integrated density was the product of the area and density. The same box was then "dragged" to the corresponding position on the superficial laminae of the dorsal horn in the spinal cord area in vgx rats, and the integrated density of pixels within the same threshold was again calculated.

Assessment of circulation parameters. Circulation parameters, including heart rate (HR), systolic blood pressure (SBP), mean blood pressure (MBP) and diastolic blood pressure (DBP), were measured by tail-cuff method (BP monitor for rat and mice model MK-2000, Muromachi Kikai, Tokyo, Japan). Measurements were performed three times in succession, and then the mean value was then calculated. In addition, measurements were performed at around the same time of day to avoid the effect of circadian rhythm.

Assessment of leakage enzyme. Blood from each rat taken from the tail vein in the presence of heparin was centrifuged at 3000 rpm to obtain plasma. The samples were stored at −20 °C until measurement and plasma concentrations of creatine phosphokinase (CPK) and lactose dehydrogenase (LDH) were measured using a Fuji Dry-Chem. analyzer (Fujifilm Medical Systems, Osaka, Japan).

Statistics. Data are presented as the mean with SEM. Statistical analysis was performed using one-way or two-way repeated-measures analysis of variance followed by a post hoc Tukey–Kramer multiple comparison test. The results of the pin-prick test was analyzed by the Mann–Whitney *U*-test. A probability level of $P<0.05$ was considered to reflect statistical significance.

RESULTS

Subdiaphragmatic vagotomy decreases the body weight

Although no significant change in body weight at baseline between groups (347±14 g vs. 350±10 g, $P=0.59$; subdiaphragmatic vagotomy vs. sham) were found, the apparent decrease of body weight following subdiaphragmatic vagotomy was observed from day 3 (339±10 g vs. 377±5 g, $P=0.004$; subdiaphragmatic vagotomy vs. sham) to day 28 (427±12 g vs. 481±8 g, $P=0.003$; subdiaphragmatic vagotomy vs. sham) after operation. This result was consistent with those in previous reports (Opsahl and Powley, 1977; Kraly et al., 1986), which indicates that the operation was successful.

Subdiaphragmatic vagotomy causes a persistent decrease in the pressure-induced withdrawal threshold of the calf

The baseline withdrawal threshold was similar in sham-operated and subdiaphragmatic vagotomized rats. Although there was still no difference in the pressure-induced withdrawal threshold between subdiaphragmatic vagotomized and sham-operated rats at 3 days after the operation, subdiaphragmatic vagotomy significantly decreased the withdrawal threshold from day 7 ($P=0.0038$) to day 28 ($P=0.0076$) after the operation, as shown in Fig. 1A.

Subdiaphragmatic vagotomy-induced hyperalgesia reflects muscle pain

To determine whether the pain in response to the application of pressure to the calves reflects cutaneous pain and/or muscle pain, we investigated the local effects of xylocaine, both intracutaneously and i.m., on the pressure stimuli-induced pain threshold.

Intracutaneous injection of 1% xylocaine decreases mechanical stimuli-induced pain. When vehicle was administered to the hind paw intracutaneously, strong noxious stimulation (pin-prick test) of the injection site caused remarkable pain-related behavior (vocalization) for up to 30 min after treatment in both sham-operated and subdiaphragmatic vagotomized rats. On the other hand, 1% xylocaine significantly suppressed pain-related behavior from 5 to 15 min in both sham-operated rats ($P=0.0027$, $P=0.0047$ and $P=0.0039$; 5, 10 and 15 min after injection) and subdiaphragmatic vagotomized rats ($P=0.0027$, $P=0.0039$ and $P=0.018$; 5, 10 and 15 min after injection), which means that the intracutaneous administration of 1% xylocaine had a local anesthetic effect on skin (Fig. 1B).

Intracutaneous injection of 1% xylocaine has no effects on the pressure-induced pain threshold of the calf. Next, we investigated the local effect of 1% xylocaine, injected at the site where pressure was applied, on the withdrawal threshold in response to the application of pressure to the calf. Ten min after the intracutaneous administration of 1%

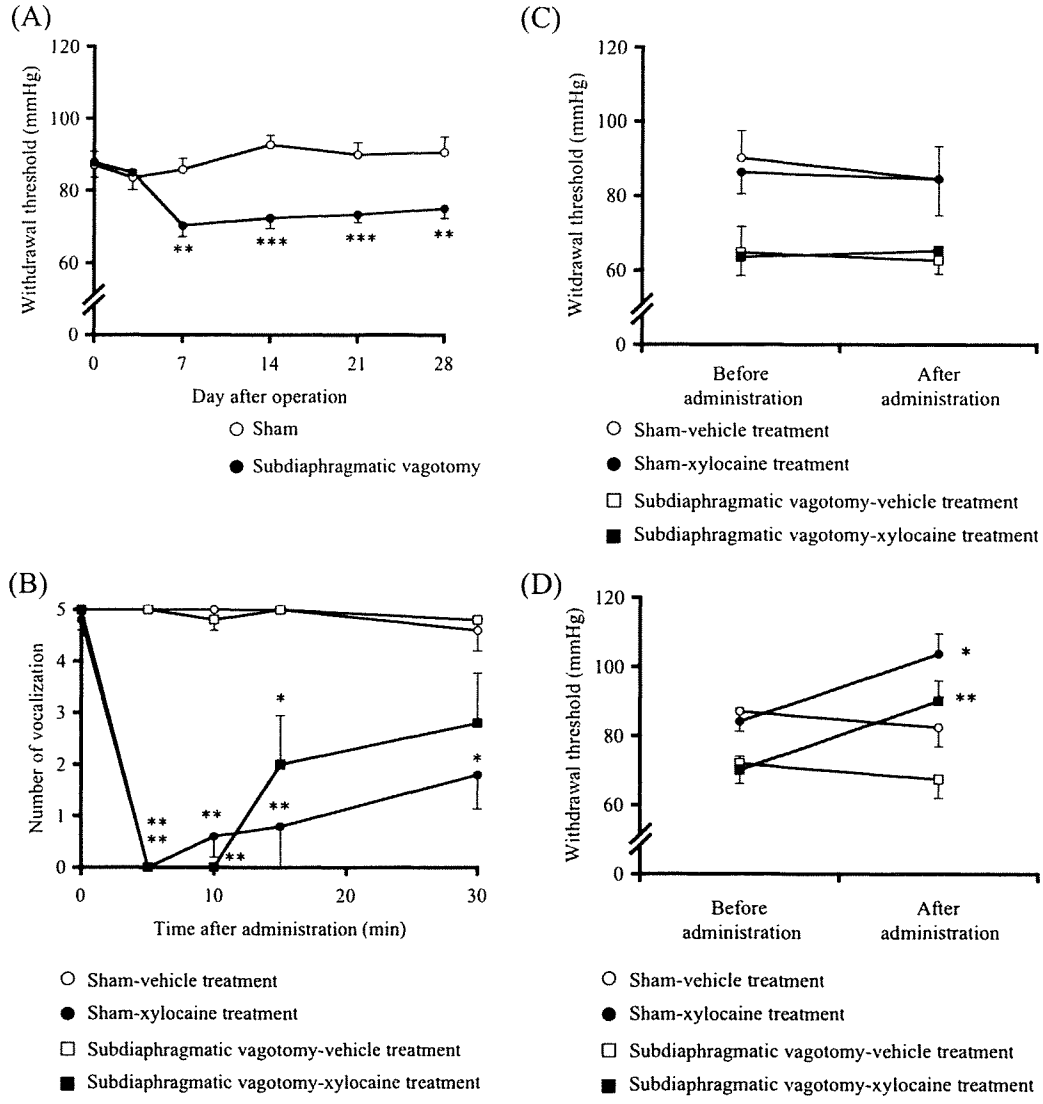

Fig. 1. Time-course of changes in pressure-induced withdrawal threshold of gastrocnemius muscle. Pressure stimuli-induced withdrawal threshold of the calf was measured by the Randall-Selitto test at 0, 3, 7, 14, 21 and 28 days after the operation (A). Subdiaphragmatic vagotomy significantly decreased the withdrawal threshold from 7 days to the end of the experiment. Values represent the mean with SEM (sham-operated rats $n=7$, subdiaphragmatic vagotomized rats $n=8$). *** $P<0.001$, ** $P<0.01$ compared to the sham-operated groups. Effects of intracutaneous (B, C) and i.m. (D) injection of 1% xylocaine on mechanical stimuli-induced pain-related behavior (B) and pressure stimuli-induced pain threshold (C, D). (B) Change (positive responses out of five stimuli) in the number of vocalizations (pain-related behavior) in both groups before and after the intracutaneous administration of 1% xylocaine. Xylocaine significantly decreased the number of vocalizations from 5 to 15 min after administration in both groups. Values represent the mean with SEM ($n=5$). ** $P<0.01$, * $P<0.05$ compared to the same operated groups after vehicle treatment. (C) Change in the withdrawal threshold in both groups before and 10 min after the intracutaneous injection of 1% xylocaine. Xylocaine had no effects on the pressure stimuli-induced withdrawal threshold in either group. Values represent the mean with SEM ($n=5$). (D) Change in the withdrawal threshold in both groups before and 30 min after the i.m. injection of 1% xylocaine. Xylocaine significantly increased the pressure stimuli-induced withdrawal threshold in both groups. Values represent the mean with SEM ($n=6$). ** $P<0.01$, * $P<0.05$ compared to the same operated groups after vehicle treatment.

xylocaine (under local anesthesia of the skin), there was no difference in the withdrawal threshold between the xylocaine- and vehicle-treated groups in both sham-operated and subdiaphragmatic vagotomized rats, as shown in Fig. 1C. These results indicate that the withdrawal threshold in response to the application of pressure to the calf does not reflect cutaneous pain under the present testing condition.

Intramuscular injection of 1% xylocaine decreases pressure-induced pain threshold of the calf. Finally, we investigated the local effect of 1% xylocaine administered into the gastrocnemius muscle on the withdrawal threshold for the application of pressure to the calf. Fig. 2D shows that, at 30 min after administration, xylocaine significantly increased the withdrawal threshold compared to the vehicle-treated group in both sham-operated and subdiaphragmatic vagotomized rats ($P=0.025$ and $P=0.0091$). These results show that the pressure stimuli-induced withdrawal threshold reflects muscle pain, but not cutaneous pain. Taken together, these results show that subdiaphragmatic vagotomy decreased the withdrawal threshold of the calf,

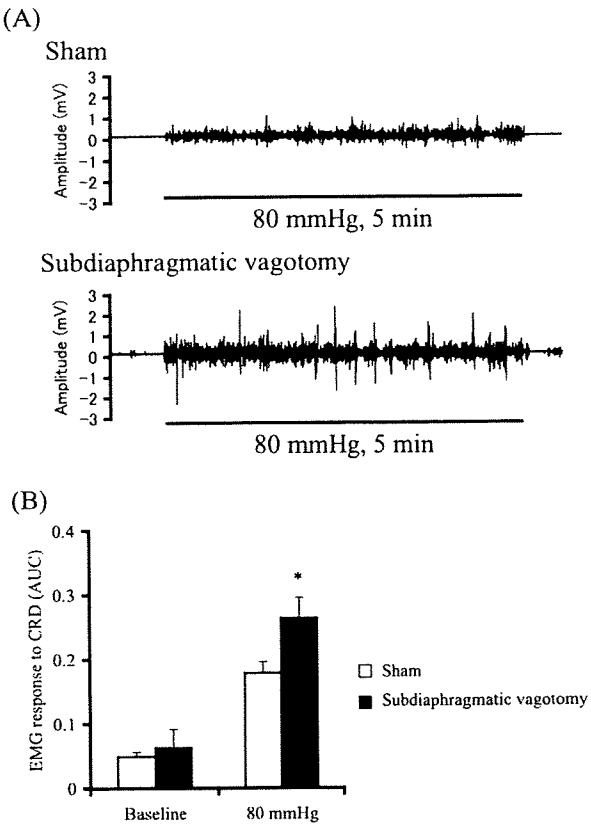

Fig. 2. Effect of subdiaphragmatic vagotomy on the visceromotor response to noxious colorectal distension. (A) Representative tracing of visceromotor responses to CRD (80 mmHg, 5 min) recorded from the external oblique muscles in sham-operated and subdiaphragmatic vagotomized rats. (B) EMG response was quantified as the mean amplitude, expressed as the AUC. Values represent the mean with SEM (sham-operated rats $n=7$, subdiaphragmatic vagotomized rats $n=6$). * $P<0.05$ compared to the sham-operated groups.

which means that subdiaphragmatic vagotomy caused chronic muscle hyperalgesia.

Subdiaphragmatic vagotomy increases visceral sensitivity

We investigated visceral sensitivity in sham-operated and subdiaphragmatic vagotomized rats by using balloon distension of the colon. Two weeks after the operation, the mean of AUC of EMG activity was significantly increased in subdiaphragmatic vagotomized rats compared to that in sham-operated rats ($P=0.03$), as shown in Fig. 2.

Subdiaphragmatic vagotomy does not modulate cutaneous both thermal and mechanical sensitivity

Two weeks after the operation, we did not detect any differences in the withdrawal latency induced by thermal (7.6±0.28 s vs. 7.5±0.34 s, $P=0.84$; subdiaphragmatic vagotomy vs. sham) and withdrawal threshold induced by mechanical-stimulus (24±4.8 g vs. 26±3.0 g, $P=0.65$; subdiaphragmatic vagotomy vs. sham) between subdiaphragmatic vagotomy and sham-operated groups.

Subdiaphragmatic vagotomy causes no tissue injury

To determine whether chronic muscle pain in subdiaphragmatic vagotomized rats is due to muscle injury, we investigated the plasma levels of CPK and LDH until the end of the examination. There were no differences in the plasma CPK and LDH levels between sham-operated and subdiaphragmatic vagotomized rats during the examination period (Table 1), which indicates that subdiaphragmatic vagotomy caused no muscle injury in the present study.

Subdiaphragmatic vagotomy disturbs the circulation

To assess the autonomic balance of subdiaphragmatic vagotomized rats, we measured circulation parameters in restrained conscious rats. While there was no difference in HR between sham-operated and subdiaphragmatic vagotomized rats, SBP, MBP and DBP were significantly increased compared to those in sham-operated rats at 1 ($P=0.032$, $P=0.0015$, $P=0.0028$, respectively) and 2 weeks ($P=0.0053$, $P=0.0059$, $P=0.016$, respectively) after surgery, as shown in Table 2.

Subdiaphragmatic vagotomy increases the expression levels of pain-related proteins within the spinal cord dorsal horn

It is well known that chronic pain is the result of plastic changes in the peripheral and central nervous system (CNS). Therefore, we investigated the levels of pain-related proteins, such as mGluR5 and PKCγ, in the spinal cord. The levels of mGluR5, PKCγ and its activated form phosphorylated-PKCγ-like immunoreactivity in lumbar 5 spinal cords of subdiaphragmatic vagotomized rats were significantly higher than those in sham-operated rats ($P=0.0061$, $P=0.041$, $P=0.0015$, respectively) (Fig. 3). These changes were particularly noted at the inner lamina II layer of the spinal cord dorsal horn.

Effects of various analgesic drugs on subdiaphragmatic vagotomy-induced muscle hyperalgesia

To determine the characteristics of chronic pain in subdiaphragmatic vagotomized rats, we investigated the effects of various analgesic drugs on subdiaphragmatic vagotomy-induced chronic muscle hyperalgesia.

Morphine. There was no difference in the analgesic effect of a higher dose of morphine between sham-operated rats and subdiaphragmatic vagotomized rats (Fig. 4A, Table 3). In contrast, a lower dose of morphine was associated with a significant increase in the withdrawal threshold of sham-operated rats at 30 min after administration ($P=0.0093$), but had no similar effects in subdiaphragmatic vagotomized rats at that time ($P=0.13$). Moreover, the %MPE of low-dose morphine at 30 min after administration in subdiaphragmatic vagotomized rats was significantly lower than that in sham-operated rats ($P=0.049$) (Fig. 4B). On the other hand, at 60 min after administration, there was no difference in the %MPE of low-dose morphine between sham-operated and subdiaphragmatic va-

Table 1. Changes in the plasma concentrations of leakage enzymes induced by subdiaphragmatic vagotomy

		Days after the operation									
		Baseline		Three		Seven		Fourteen		Twenty-eight	
Parameter	Unit	Sham	Subdiaphragmatic vagotomy	Sham	Subdiaphragmatic vagotomy	Sham	Subdiaphragmatic vagotomy	Sham	Subdiaphragmatic vagotomy	Sham	Subdiaphragmatic vagotomy
CPK	U/L	285±24	431±107	271±29	210±26	291±43	331±61	528±159	622±172	777±173	741±252
LDH	U/L	384±57	391±35	392±84	210±22	230±48	153±53	108±16	122±21	189±40	123±24

Plasma concentrations of LDH and CPK at baseline, 3, 7, 14 and 28 days after the operation were measured in sham-operated and subdiaphragmatic vagotomized groups. Each data represents the mean with SEM of six to eight animals.

gotomized rats (Fig. 4C), and the $AUC_{0\text{-}60\,min}$ of the %MPE of low-dose morphine in subdiaphragmatic vagotomy tended to be less than that in sham-operated rats, albeit this difference was not significant ($P=0.085$) (Fig. 4D).

Diclofenac and dexamethasone. No significant difference was noted between the vehicle- and diclofenac (non-steroidal anti-inflammatory drug)-treated groups in both sham-operated and subdiaphragmatic vagotomized rats, as shown in Table 3.

The steroidal anti-inflammatory drug dexamethasone, 60 min after i.v. administration at 1 mg/kg, also had no effects on the withdrawal threshold in either group, as shown in Table 3.

Gabapentin and amitriptyline. Although single s.c. administrations of gabapentin at 30 mg/kg and amitriptyline at 10 mg/kg caused no changes in the withdrawal threshold in sham-operated rats, gabapentin 1 h after administration and amitriptyline 3 h after administration significantly increased the withdrawal threshold in subdiaphragmatic vagotomized rats compared to that in the vehicle-treated group ($P=0.0027$ and $P=0.0098$, gabapentin and amitriptyline, respectively) (Table 3).

Diazepam. As shown in Table 3, 30 min after the s.c. administration of diazepam at 2 mg/kg, there was no difference in the withdrawal threshold between sham-operated and subdiaphragmatic vagotomized rats.

DISCUSSION

The present study is the first to demonstrate that subdiaphragmatic vagotomized rats showed delayed and sustained muscle hyperalgesia accompanied by visceral hypersensitivity. Subdiaphragmatic vagotomy itself caused no tissue injury because there were no changes in CPK and LDH, indicators of muscle injury, between sham-operated and subdiaphragmatic vagotomized rats, and anti-inflammatory drugs such as diclofenac and dexamethasone were not effective on subdiaphragmatic vagotomy-induced pain. In our preliminary study, we did not find any changes in the number of white blood cells induced by subdiaphragmatic vagotomy until 4 weeks after operation (data not shown). Therefore, it was supposed that subdiaphragmatic vagotomy-induced chronic muscle pain might be caused by nociceptive plasticity, but not by muscle damage. To identify whether pain-related protein levels are increased in the spinal cord under subdiaphragmatic vagotomy, we investigated the expression levels of mGluR5, PKCγ, and phosphorylated-PKCγ in lumbar 5 (L5) spinal cord segment, which transmits a nociceptive signal from the gastrocnemius muscle (Panneton et al., 2005). We previously reported that neuropathic pain following chronic ethanol consumption increased the expression levels of mGluR5 and conventional phosphorylated-PKC, including PKCγ, in the superficial dorsal horn of the spinal cord (Miyoshi et al., 2006; Narita et al., 2007). In addition, both mGluR5 and PKC inhibitors suppressed mechanical hyperalgesia in chronic ethanol consumption induced-neuro-

Table 2. Changes in circulation parameters during muscle hyperalgesia

Parameter	Unit	One wk after the operation		Two wk after the operation	
		Sham	Subdiaphragmatic vagotomy	Sham	Subdiaphragmatic vagotomy
HR	beats/min	364±8.9	376±9.1	353±8.7	363±11.2
SBP	mmHg	120±3.1	135±6.2*	114±2.0	125±5.4**
MBP	mmHg	86±3.3	106±4.0**	80±1.2	98±5.4**
DBP	mmHg	69±4.7	90±3.8**	63±1.4	76±4.6*

HR, SBP, MBP and DBP were measured in conscious rats at 1 and 2 wk after the operation by the tail-cuff method.
Each column represents the mean with SEM of eight to eleven animals.
** $P<0.01$, * $P<0.05$ compared to the sham-operated group.

pathic pain in rats (Miyoshi et al., 2007). Among all of the PKC subtypes, PKCγ in the spinal cord plays an important role in the development of a state of neuropathic pain, but not involved in chronic inflammatory pain (Malmberg et al., 1997; Ohsawa et al., 2000). In the present study, our immunohistochemical data demonstrated that the levels of mGluR5, PKCγ and phosphorylated-PKCγ were dramatically increased in the superficial dorsal horn of the L5 spinal cord segment, especially lamina II inner part, which is central termination of sensory fibers from nerves to the gastrocnemius muscle (Panneton et al., 2005), in subdiaphragmatic vagotomized rats. These results support the notion that subdiaphragmatic vagotomy causes nociceptive plasticity in the CNS. Although it is well known that the main expression site of PKCγ is laminae II and III (Polgár et al., 1999), phosphorylated-PKCγ was also detected in lamina I at the present study. This is due to the multiplicity of antibodies used in the present study, since the commercially available phosphorylated-PKCγ antibody used in the present study slightly detects other PKC subtypes.

Although we did not focus on the detailed mechanism of subdiaphragmatic vagotomy-induced pain in the present study, we here propose its possible mechanism through both peripheral and central pathways as follows. At first, chronic relative sympathetic nerve activation after subdiaphragmatic vagotomy may contribute to its related chronic pain. Khasar et al. (1998a) revealed that adrenalectomy or adrenal denervation prevented subdiaphragmatic vagotomy-induced mechanical hyperalgesia in rats. They suggested that subdiaphragmatic vagotomy-induced hyperalgesia could be caused by a sympatho-adrenal-dependent mechanism via an excessive release of hormone, but not via epinephrine release. In the present study, subdiaphragmatic vagotomized rats exhibited high blood pressure conditions, which means that relative sympathetic nerve activation may be occurred in subdiaphragmatic vagotomized rats. Secondly, subdiaphragmatic vagotomy may cause the sustained suppression of descending pain-inhibitory pathways, which promotes pain sensitivity of muscle and distal colon, because vagal afferents terminates in the nucleus of the solitary tract, that comprises a relay to many brain areas including the rostral ventral medulla (RVM) (Kalia and Sullivan, 1982; Randich et al., 1990; Ren et al., 1990). The descending pain-inhibitory pathways from RVM represent an important supraspinal mechanism in modulating spinal nociceptive transmission (Urban and Gebhart, 1997). Finally, the decreases of signal transduction of gastrointestinal peptides to the CNS via the vagus afferent may play an important role in subdiaphragmatic vagotomy-induced pain. Ghrelin, one of the gastrointestinal peptide, was isolated from the rat stomach as an endogenous ligand for the growth hormone secretagogue receptor (Kojima et al., 1999). Date et al. (2001, 2002) has reported that the gastric vagal afferent is the major pathway conveying ghrelin's signals for starvation and growth hormone secretion to the brain for promoting increased food intake. They have also showed that ghrelin activates neuropeptide Y (NPY)-producing neurons in the arcurate nucleus via the vagus afferent, and the administration of NPY to the arcurate nucleus induces a dose-dependent antinociception in both intact rats and rats with inflammation (Li et al., 2005). Thus, inhibition of peripheral signal transduction by ghrelin via the vagus afferent may contribute to inhibition of NPY secretion in the arcurate nucleus, causing chronic pain.

It was reported that the analgesic effect of morphine in subdiaphragmatic vagotomized rats at the early phase after administration was weaker than that in sham-operated rats, based on the results in the tail-flick test (Randich et al., 1991), which agrees with the results in the present study. Moreover, μ opioid receptors are present in vagal afferents (Aicher et al., 2000). These findings support the idea that μ opioid receptor in the vagal nerve may be involved in the opioid-induced analgesic effect at the early phase after administration.

It is not definite why blood concentration of CPK was gradually increased in the present study. However, Heffron and Mitchell (1975) reported a good correlation between increase rate of body weight and serum concentration of CPK release, indicating that serum concentration of CPK could be age-dependently changed.

In this study, we demonstrated that (i) subdiaphragmatic vagotomy caused chronic muscle pain accompanied by visceral hypersensitivity, (ii) subdiaphragmatic vagotomy-induced muscle pain was attenuated by gabapentin and amitriptyline, but not by diclofenac or dexamethasone, and was partially suppressed by a lower dose of morphine, and (iii) subdiaphragmatic vagotomy caused relative sympathetic nerve activation without muscle damage in subdiaphragmatic vagotomized rats. Similar phenomena have been noted in fibromyalgia syndrome (FMS) patients. FMS is a disorder that results in generalized chronic pain for sufferers and is defined by the American College of Rheumatology as chronic widespread muscle pain (Wolfe

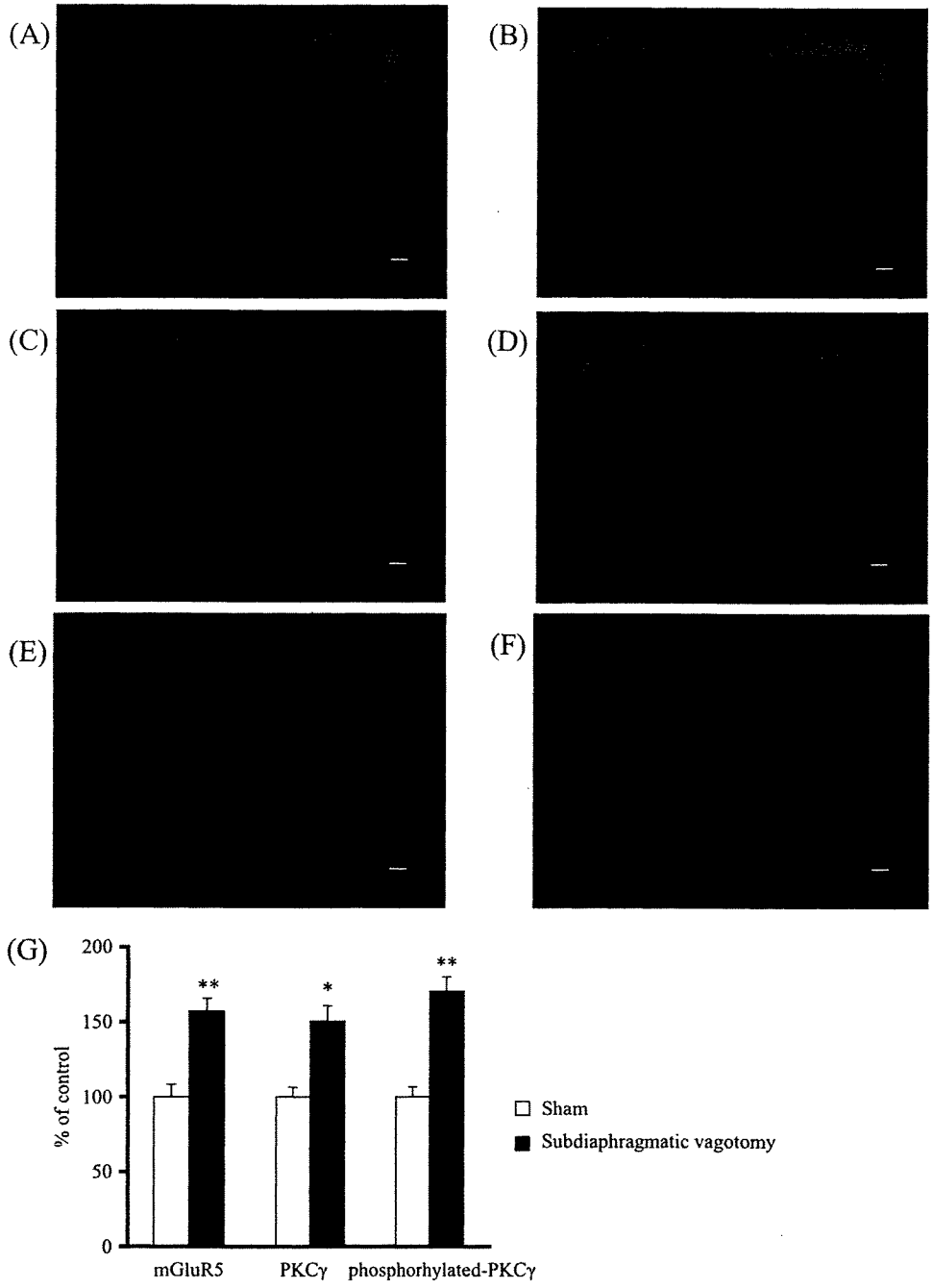

Fig. 3. Change in the levels of mGluR5, PKC γ- and phosphorylated-PKCγ-like immunoreactivities (IRs) in the superficial dorsal horn of the rat spinal cord after subdiaphragmatic vagotomy. The levels of mGluR5-IR (A, B, sham-operated group and subdiaphragmatic vagotomy, respectively), PKCγ-IR (C, D, sham-operated group and subdiaphragmatic vagotomy, respectively), and phosphorylated-PKCγ-IR (E, F, sham-operated group and subdiaphragmatic vagotomy, respectively) in the superficial dorsal horn of the rat spinal cord were increased after subdiaphragmatic vagotomy. (A–F) Two weeks after the operation, animals were perfused with 4% formalin, tissue was incubated in sucrose buffer for 3 days, and frozen tissue was cut into 10 mm-thick coronal sections using a cryostat. Specimens were then incubated in specific primary antibodies for 48 h, and then with secondary antibodies. Images were obtained with a fluorescence microscope and edited with Adobe Photoshop™. (G) Semi-quantitative analysis was performed using NIH Image, which showed significant increases in mGluR5, PKCγ and phosphorylated-PKCγ in subdiaphragmatic vagotomized rats. Values represent the mean with SEM (n=3). ** P<0.01, * P<0.05 compared to the sham-operated group. Scale bars: 100 μm. For interpretation of the references to color in this figure legend, the reader is referred to the Web version of this article.

et al., 1990). Its principal symptoms are the appearance of a number of tender points around the body, stiffness in the muscles, tendons and surrounding soft tissue, weakness, sleep disorders, disturbances in bowel function, rigidity in the extremities, and depressive episodes accompanied by anxiety crises (Wolfe, 2003). Epidemiologic investigations have revealed that approximately 2% of the worldwide population may suffer from FMS (Wolfe et al., 1995) and

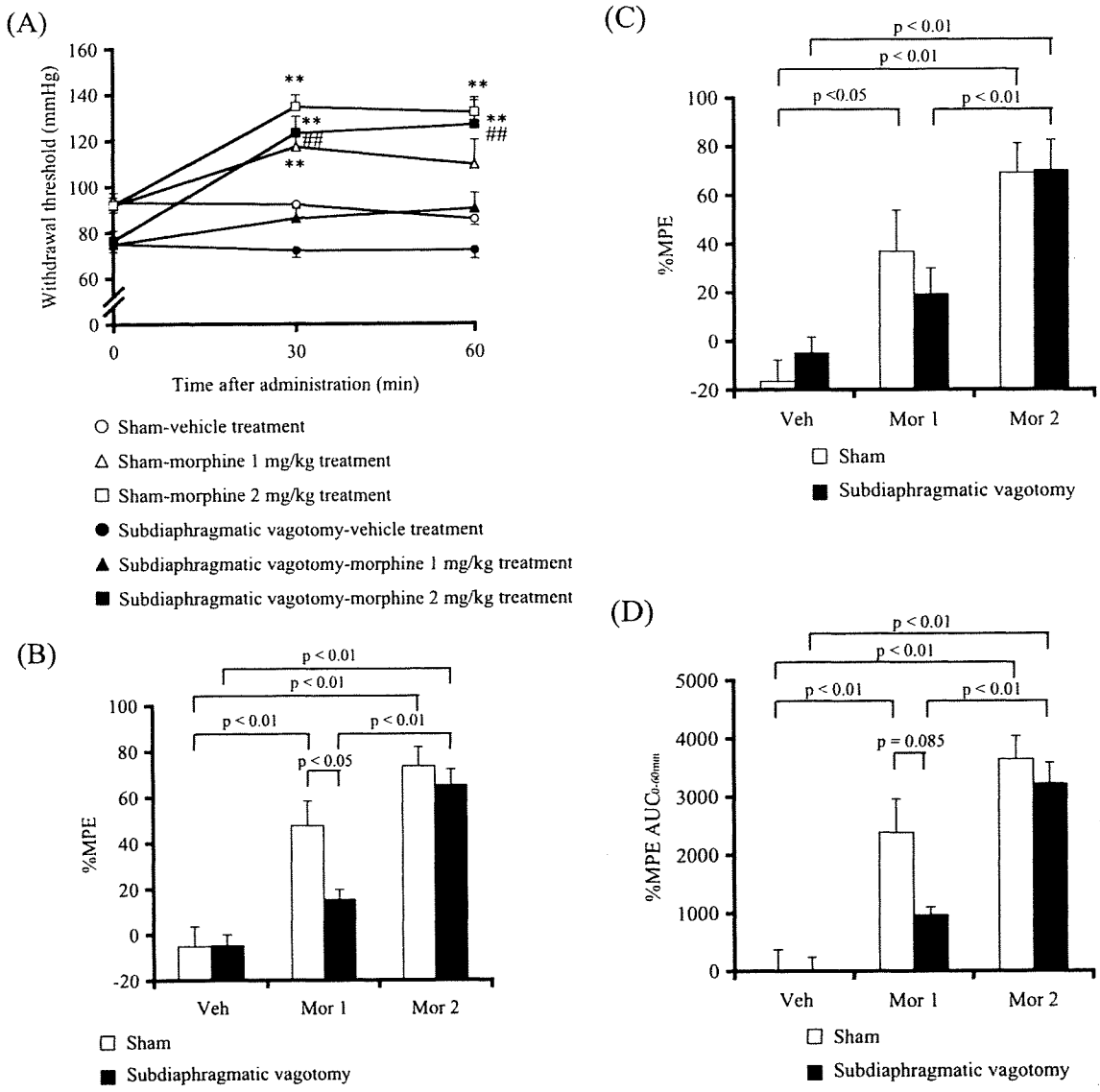

Fig. 4. Effects of morphine on subdiaphragmatic vagotomy-induced muscle hyperalgesia. The muscle withdrawal threshold was measured by the Randall-Selitto test before and after morphine administration (A). % MPE of morphine was obtained at 30 minutes (B), 60 minutes (C) after administration, and $AUC_{0\text{-}60\ min}$ (D). % MPE was calculated using the following formula; (post-administration withdrawal threshold—pre-administration withdrawal threshold)/(150 mmHg (cut-off value)—pre-administration withdrawal threshold). The extent and duration of antinociception were quantified by calculating the AUC using trapezoidal integration. Each data point represents the mean with SEM of six to eight animals. ** $P<0.01$, * $P<0.05$ compared to the same operated group after vehicle treatment. ## $P<0.01$ compared to the same operated group after low-dose morphine treatment. Veh, vehicle treatment; Mor 1, morphine 1 mg/kg treatment; Mor 2, morphine 2 mg/kg treatment.

many patients still suffer from a poor quality of life (Burckhardt et al., 1993). In particular, (i) FMS is a disease of chronic musculoskeletal pain that is complicated by irritable bowel syndrome, for which the main symptom is abdominal pain, (ii) gabapentin and amitriptyline are effective against pain in FMS patients (Arnold et al., 2007; Uçeyler et al., 2008), while anti-inflammatory drugs have no effect (Clark et al., 1985; Yunus et al., 1989), and opioids are relatively ineffective (Rao and Clauw, 2004), and (iii) FMS patients fail to show apparent abnormal findings (Undeland and Malterud, 2007), and show activation of the sympathetic nervous system (Martinez-Lavin, 2007). These common phenomena suggest that subdiaphragmatic vagotomy-induced chronic pain reflects, at least in part, FMS symptoms.

CONCLUSION

In conclusion, the present results suggest that subdiaphragmatic vagal dysfunction may be a risk factor for the development of chronic muscle pain accompanied by visceral hypersensitivity and sympathetic hyperactivity, which are partially similar to the symptoms of FMS. Furthermore,

Table 3. Effects of various analgesic drugs on subdiaphragmatic vagotomy

			Sham				Subdiaphragmatic vagotomy			
			Time after administration				Time after administration			
Drug	Dose	Route	Before	Half an hour	One hour	Three hour	Before	Half an hour	One hour	Three hour
Vehicle		s.c.	94±4.8	92±2.1	87±3.0		76±3.8	74±3.1	73±4.2	
Morphine	1 mg/kg	s.c.	94±6.1	119±8.5**	114±11.5		77±1.7	89±4.5	91±7.8	
Morphine	2 mg/kg	s.c.	94±3.5	132±5.6**	132±7.8**		81±2.2	130±3.8**##	135±7.4**##	
Vehicle		s.c.	100±5.3	95±4.8			78±1.6	78±4.4		
Diclofenac	3 mg/kg	s.c.	97±4.6	103±6.8			75±2.4	82±5.2		
Vehicle		i.v.	101±3.3		98±2.5		79±5.3		79±1.3	
Dexamethasone	1 mg/kg	i.v.	100±4.2		99±3.0		77±3.4		79±2.1	
Vehicle		s.c.	107±9.7	106±9.6			82±4.4	78±2.4		
Diazepam	2 mg/kg	s.c.	108±5.5	106±8.5			78±3.8	78±5.5		
Vehicle		s.c.	103±5.9		98±3.1		78±1.8		74±1.5	
Gabapentin	30 mg/kg	s.c.	100±7.4		93±4.2		79±1.7		96±3.6**	
Vehicle		s.c.	97±3.2		100±2.8	101±2.2	80±1.5		82±2.6	82±1.8
Amitriptyline	10 mg/kg	s.c.	103±2.9		93±1.9	100±3.4	81±1.9		92±4.1	93±3.2**

The muscle withdrawal threshold was measured by the Randall-Selitto test before and after drug administration.
Each data point represents the mean with SEM of five to eight animals.
** $P<0.01$ compared to the same operated group after vehicle treatment.
$P<0.01$ compared to the same operated group after low-dose morphine treatment.

this muscle pain may result from nociceptive neuroplasticity of the spinal cord dorsal horn.

Acknowledgments—This work was supported in part by grants from the Ministry of Health, Labor and Welfare and the Ministry of Education, Culture, Sports, Science and Technology of Japan. We wish to thank Keiichi Niikura Ph.D., Keisuke Hashimoto Ph.D., Yasuhisa Kobayashi M.B., Mahardian Rahmadi B.S., Masaharu Furuya B.S., Tetsuo Nakano M.B. and Aya Saito D.V.M. for their expert technical assistance. The authors declare no conflict of interest.

REFERENCES

Aicher SA, Goldberg A, Sharma S, Pickel VM (2000) Mu-opioid receptors are present in vagal afferents and their dendritic targets in the medial nucleus tractus solitarius. J Comp Neurol 422:181–190.

Arnold LM, Goldenberg DL, Stanford SB, Lalonde JK, Sandhu HS, Keck PE Jr, Welge JA, Bishop F, Stanford KE, Hess EV, Hudson JI (2007) Gabapentin in the treatment of fibromyalgia: a randomized, double-blind, placebo-controlled, multicenter trial. Arthritis Rheum 56:1336–1344.

Beyreuther B, Callizot N, Stöhr T (2006) Antinociceptive efficacy of lacosamide in a rat model for painful diabetic neuropathy. Eur J Pharmacol 539:64–70.

Burckhardt CS, Clark SR, Bennett RM (1993) Fibromyalgia and quality of life: a comparative analysis. J Rheumatol 20:475–479.

Buritova J, Honoré P, Chapman V, Besson JM (1996) Enhanced effects of co-administered dexamethasone and diclofenac on inflammatory pain processing and associated spinal c-Fos expression in the rat. Pain 64:559–568.

Chen SL, Wu XY, Cao ZJ, Fan J, Wang M, Owyang C, Li Y (2008) Subdiaphragmatic vagal afferent nerves modulate visceral pain. Am J Physiol Gastrointest Liver Physiol 294:G1441–G1449.

Clark S, Tindall E, Bennett RM (1985) A double blind crossover trial of prednisone versus placebo in the treatment of fibrositis. J Rheumatol 12:980–983.

Date Y, Murakami N, Toshinai K, Matsukura S, Niijima A, Matsuo H, Kangawa K, Nakazato M (2002) The role of the gastric afferent vagal nerve in ghrelin-induced feeding and growth hormone secretion in rats. Gastroenterology 123:1120–1128.

Date Y, Nakazato M, Murakami N, Kojima M, Kangawa K, Matsukura S (2001) Ghrelin acts in the central nervous system to stimulate gastric acid secretion. Biochem Biophys Res Commun 280: 904–907.

Esser MJ, Sawynok J (1999) Acute amitriptyline in a rat model of neuropathic pain: differential symptom and route effects. Pain 80:643–653.

Fujii Y, Ozaki N, Taguchi T, Mizumura K, Furukawa K, Sugiura Y (2008) TRP channels and ASICs mediate mechanical hyperalgesia in models of inflammatory muscle pain and delayed onset muscle soreness. Pain 140:292–304.

Gschossmann JM, Mayer EA, Miller JC, Raybould HE (2002) Subdiaphragmatic vagal afferent innervation in activation of an opioidergic antinociceptive system in response to colorectal distension in rats. Neurogastroenterol Motil 14:403–408.

Heffron JJ, Mitchell G (1975) Age dependent variation of serum creatine phosphokinase levels in pigs. Experientia 31:657–658.

Holtmann G, Goebell H, Jockenhoevel F, Talley NJ (1998) Altered vagal and intestinal mechanosensory function in chronic unexplained dyspepsia. Gut 42:501–506.

Kalia M, Sullivan JM (1982) Brainstem projections of sensory and motor components of the vagus nerve in the rat. J Comp Neurol 211:248–265.

Khasar SG, Miao FJ, Jänig W, Levine JD (1998a) Vagotomy-induced enhancement of mechanical hyperalgesia in the rat is sympathoadrenal-mediated. J Neurosci 18:3043–3049.

Khasar SG, Miao JP, Jänig W, Levine JD (1998b) Modulation of bradykinin-induced mechanical hyperalgesia in the rat by activity in abdominal vagal afferents. Eur J Neurosci 10:435–444.

Kojima M, Hosoda H, Date Y, Nakazato M, Matsuo H, Kangawa K (1999) Ghrelin is a growth-hormone-releasing acylated peptide from stomach. Nature 402:656–660.

Kraly FS, Jerome C, Smith GP (1986) Specific postoperative syndromes after total and selective vagotomies in the rat. Appetite 7:1–17.

Li JJ, Zhou X, Yu LC (2005) Involvement of neuropeptide Y and Y1 receptor in antinociception in the arcuate nucleus of hypothalamus,

an immunohistochemical and pharmacological study in intact rats and rats with inflammation. Pain 118:232–242.
Malmberg AB, Chen C, Tonegawa S, Basbaum AI (1997) Preserved acute pain and reduced neuropathic pain in mice lacking PKCγ. Science 278:279–283.
Martinez-Lavin M (2007) Biology and therapy of fibromyalgia. Stress, the stress response system, and fibromyalgia. Arthritis Res Ther 9:216.
Miyoshi K, Narita M, Narita M, Suzuki T (2006) Involvement of mGluR5 in the ethanol-induced neuropathic pain-like state in the rat. Neurosci Lett 410:105–109.
Miyoshi K, Narita M, Takatsu M, Suzuki T (2007) mGlu5 receptor and protein kinase C implicated in the development and induction of neuropathic pain following chronic ethanol consumption. Eur J Pharmacol 562:208–211.
Munro G, Lopez-Garcia JA, Rivera-Arconada I, Erichsen HK, Nielsen EO, Larsen JS, Ahring PK, Mirza NR (2008) Comparison of the novel subtype selective GABAA receptor positive allosteric modulator NS11394 with diazepam, zolpidem, bretazenil and gaboxadol in rat models of inflammatory and neuropathic pain. J Pharmacol Exp Ther 327:969–981.
Narita M, Miyoshi K, Narita M, Suzuki T (2007) Changes in function of NMDA receptor NR2B subunit in spinal cord of rats with neuropathy following chronic ethanol consumption. Life Sci 80:852–859.
Ness TJ, Gebhart GF (1988) Colorectal distension as a noxious visceral stimulus: physiologic and pharmacologic characterization of pseudaffective reflexes in the rat. Brain Res 450:153–169.
Ohsawa M, Narita M, Mizoguchi H, Suzuki T, Tseng LF (2000) Involvement of spinal protein kinase C in thermal hyperalgesia evoked by partial sciatic nerve ligation, but not by inflammation in the mouse. Eur J Pharmacol 403:81–85.
Opsahl CA, Powley TL (1977) Body weight and gastric acid secretion in rats with subdiaphragmatic vagotomy and lateral hypothalamic lesions. J Comp Physiol Psychol 91:1284–1296.
Panneton WM, Gan Q, Juric R (2005) The central termination of sensory fibers from nerves to the gastrocnemius muscle of the rat. Neuroscience 134:175–187.
Polgár E, Fowler JH, McGill MM, Todd AJ (1999) The types of neuron which contain protein kinase C gamma in rat spinal cord. Brain Res 833:71–80.
Raghavendra V, Rutkowski MD, DeLeo JA (2002) The role of spinal neuroimmune activation in morphine tolerance/hyperalgesia in neuropathic and sham-operated rats. J Neurosci 22:9980–9989.
Randall LO, Selitto JJ (1957) A method for measurement of analgesic activity on inflamed tissue. Arch Int Pharmacodyn Ther 111:409–419.
Randich A, Gebhart GF (1992) Vagal afferent modulation of nociception. Brain Res Brain Res Rev 17:77–99.
Randich A, Ren K, Gebhart GF (1990) Electrical stimulation of cervical vagal afferents. II. Central relays for behavioral antinociception and arterial blood pressure decreases. J Neurophysiol 64:1115–1124.
Randich A, Thurston CL, Ludwig PS, Timmerman MR, Gebhart GF (1991) Antinociception and cardiovascular responses produced by intravenous morphine: the role of vagal afferents. Brain Res 543:256–270.
Rao SG, Clauw DJ (2004) The management of fibromyalgia. Drugs Today (Barc) 40:539–554.
Ren K, Randich A, Gebhart GF (1988) Vagal afferent modulation of a nociceptive reflex in rats: involvement of spinal opioid and monoamine receptors. Brain Res 446:285–294.
Ren K, Randich A, Gebhart GF (1990) Electrical stimulation of cervical vagal afferents. I. Central relays for modulation of spinal nociceptive transmission. J Neurophysiol 64:1098–1114.
Sedan O, Sprecher E, Yarnitsky D (2005) Vagal stomach afferents inhibit somatic pain perception. Pain 113:354–359.
Tal M, Bennett GJ (1994) Extra-territorial pain in rats with a peripheral mononeuropathy: mechano-hyperalgesia and mechano-allodynia in the territory of an uninjured nerve. Pain 57:375–382.
Tonussi CR, Ferreira SH (1994) Mechanism of diclofenac analgesia: direct blockade of inflammatory sensitization. Eur J Pharmacol 251:173–179.
Uçeyler N, Häuser W, Sommer C (2008) A systematic review on the effectiveness of treatment with antidepressants in fibromyalgia syndrome. Arthritis Rheum 59:1279–1298.
Undeland M, Malterud K (2007) The fibromyalgia diagnosis: hardly helpful for the patients? A qualitative focus group study. Scand J Prim Health Care 25:250–255.
Urban MO, Gebhart GF (1997) Characterization of biphasic modulation of spinal nociceptive transmission by neurotensin in the rat rostral ventromedial medulla. J Neurophysiol 78:1550–1562.
Urban MO, Ren K, Park KT, Campbell B, Anker N, Stearns B, Aiyar J, Belley M, Cohen C, Bristow L (2005) Comparison of the antinociceptive profiles of gabapentin and 3-methylgabapentin in rat models of acute and persistent pain: implications for mechanism of action. J Pharmacol Exp Ther 313:1209–1216.
Wolfe F (2003) Pain extent and diagnosis: development and validation of the regional pain scale in 12,799 patients with rheumatic disease. J Rheumatol 30:369–378.
Wolfe F, Ross K, Anderson J, Russell IJ, Hebert L (1995) The prevalence and characteristics of fibromyalgia in the general population. Arthritis Rheum 38:19–28.
Wolfe F, Smythe HA, Yunus MB, Bennett RM, Bombardier C, Goldenberg DL, Tugwell P, Campbell SM, Abeles M, Clark P, Fam AD, Farber SJ, Fiechtner JJ, Franklin CM, Gatter RA, Hamaty D, Lessard J, Lichtbroun AS, Masi AT, Mcclain GA, Reynolds WJ, Romano TH, Russel IJ, Sheon RP (1990) The American College of Rheumatology 1990 Criteria for the Classification of Fibromyalgia. Report of the Multicenter Criteria Committee. Arthritis Rheum 33:160–172.
Yunus MB, Masi AT, Aldag JC (1989) Short term effects of ibuprofen in primary fibromyalgia syndrome: a double blind, placebo controlled trial. J Rheumatol 16:527–532.

(Accepted 10 September 2009)
(Available online 20 September 2009)

SYNAPSE 63:365–368 (2009)

Direct Evidence for the Up-regulation of Vps34 Regulated by PKCγ During Short-Term Treatment With Morphine

MASAHIRO SHIBASAKI, KAZUHIRO KUROKAWA, MASASHI KATSURA, AND SEITARO OHKUMA*
Department of Pharmacology, Kawasaki Medical School, Matsushima, Kurashiki 701-0192, Japan

KEY WORDS synaptic plasticity; trafficking; μ-opioid receptor; PI 3-kinase

ABSTRACT In this study, we investigated whether PKCγ could be associated with functional changes of vacuolar protein sorting 34 (Vps34) during morphine treatment using primary cultures of cerebral cortical neurons from mice. The immunoprecipitation analysis showed that p-PKCγ and Vps34 are present together in molecular complexes. The treatment with morphine increases PKCγ and Vps34 levels. Phosphorylation of PKCγ increased Vps34 level. The inhibition of morphine-induced increase in PKCγ phosphorylation reduced Vps34 level. These results indicates that opioid receptor activation increases PKCγ phosphorylation in the neurons and, in turn, upregulates Vps34 during short-term treatment with neurons. **Synapse 63:365–368, 2009.** ©2009 Wiley-Liss, Inc.

INTRODUCTION

Vacuolar protein sorting 34 (Vps34) is the sole Class III enzyme in phosphoinositide (PI) 3-kinase family phosphorylating 3′ hydroxy position of the phosphatidylinositol ring, and selectively catalyzes phosphatidylinositol to produce only PI(3)P (Herman et al., 1992; Volinia et al., 1995). PIs play several roles including regulation of membrane trafficking in cells (De Matteis and Godi, 2004). Early endosome trafficking requires PI 3-kinase activity, and dominant kinase in this organelle appears to be human homologue of Vps34 (hVps34) (De Matteis and Godi, 2004; Futter et al., 2001). However, little is known about functions of Vps34 in opioid receptor activation by morphine.

Repeated administration of morphine produces several long-lasting changes in brain function such as protein kinase C (PKC) upregulation in the nucleus accumbens (Aoki et al., 2004; Narita et al., 2002). PKC family controls numerous signaling cascades by phosphorylation of target proteins including neurotransmitter receptors and G proteins (Hug and Sarre, 1993; Premont et al., 1995). Recent investigations demonstrate neuronal cytoplasmic localization of PKCγ in soma including dendritic spines, axon and synaptic terminals (Kose et al., 1988, 1990) and modulatory roles of PKC in calcium channel trafficking via insertion of channels into the plasma membrane (Zhang et al., 2008). In addition, our preliminary data showed that morphine (0.3 μM for 24 h) exposure to the primary cultures of cerebrocortical neurons upregulated calcium channel protein levels in neuronal plasma membrane, whereas mRNA levels of calcium channel subunits did not change (data not shown). Taken together with these data it is suggested that functional interaction between PKCγ and Vps34 may occur and regulate mechanisms of trafficking of calcium channel subunits during morphine treatment. In this study, we therefore investigated whether PKCγ could be associated with functional changes of Vps34 during morphine exposure to the primary cultures of cerebrocortical neurons.

MATERIALS AND METHODS

Isolation and primary culture of cerebral cortical neurons were carried out according to the method described earlier (Ohkuma et al., 1986). In short, the neopallium free of the meninges was removed from 15-day-old fetus of ddY mouse (Japan SLC, Hamamatsu, Japan), minced, dispersed by trypsin, and centrifuged at 1000*g*. Thereafter, the isolated cells were cultured at 37°C in humidified 95% air/5% CO_2 for 3 days. After the treatment of 10 μM cytosine arabinoside for 24 h, the neurons were used on the 13th day of the culture.

Contract grant sponsor: The Ministry of Education, Culture, Sports, Science, and Technology of Japan; Contract grant sponsor: Kawasaki Medical University.

*Correspondence to: Seitaro Ohkuma, M.D. Ph.D., Department of Pharmacology, Kawasaki Medical School, 577 Matsushima, Kurashiki 701-0192, Japan. E-mail: sohkuma@bcc.kawasaki-m.ac.jp

Received 12 June 2008; Revised 14 August 2008; Accepted 26 August 2008

DOI 10.1002/syn.20612

Published online in Wiley InterScience (www.interscience.wiley.com).

Fractions containing membranes and cytosol (S1) and endoplasmic reticulum plus Golgi complexes (microsomes, MI) were prepared from the neurons by sucrose density gradient centrifugation as described earlier (Noble et al., 2000) with a minor modification. All sucrose solutions contained 10 mM Tris-HCl (pH 7.4), 0.5 mM EDTA, 10 mM NaF, 0.5% Triton X-100 with a protease inhibitor cocktail (Roche Diagnostics, Indianapolis, IN). The neurons were homogenized and centrifuged at 1000*g* for 10 min. Resultant supernatant (S1) was centrifuged at 20,000*g* for 1 h to yield the supernatant (S2), and S2 was centrifuged at 100,000*g* for 1 h to obtain the crude microsomal pellet (P3). The P3 was resuspended in 10% sucrose, and this formed the top of a two-step gradient of 10%/28.5% sucrose solutions. Following centrifugation at 100,000*g* for 2 h, the 10%/28.5% interface was collected (MI).

Cell extracts were subjected to immunoprecipitation for 2 h using 5 μg of anti-p-PKCγ polyclonal antibodies and 25 μl of protein G-conjugated agarose beads (GE Healthcare UK Ltd., Buckinghamshire, UK) at 4°C. The beads were washed three times with 1 ml of washing buffer [10 mM Tris-HCl (pH 7.4), 0.5 mM EDTA, 10 mM NaF, 0.5% Triton X-100 with a protease inhibitor cocktail]. Proteins bound to the beads were eluted with SDS/PAGE sample buffer and subjected to immunoblotting as described later. The antibody against Vps34 did not work for immunoprecipitation.

Protein concentration in the samples was assayed by the method of Lowry et al. (1951). PKCγ and Vps34 protein extracts in S1 and MI fractions were separated by SDS-PAGE on a 7.5% acrylamide gel to transfer to nitrocellulose membranes. The membrane was incubated with primary antibody diluted in PBS (1:1000 for p-PKCγ, Stressgen Bioreagents Limited Partnership, Victoria, B.C., Canada; 1:1000 for Vps34, Zymed Labs, S. San Francisco, CA) overnight at 4°C. Thereafter, the membrane was washed and incubated for 2 h at room temperature with horseradish peroxidase-conjugated goat anti-rabbit IgG diluted 1:5000 in PBS. Immunoblots were detected with chemiluminescence detection (ECL) reagents (GE Healthcare UK Ltd., Buckinghamshire, UK).

Phorbol 12, 13-dibutyrate (PDBu) and chelerythrine chloride (CHL) were obtained from Sigma-Aldrich Co., (St. Louis). Morphine hydrochloride was a product of Sankyo Co. (Tokyo, Japan). The data were expressed as the mean ± SEM. The statistical significance was assessed by the methods described in each figure legend following the application of the one-way ANOVA.

RESULTS

Using S1 extracts from the neurons, the well-characterized antibody against phospho-Thr514 of PKCγ immunoprecipitated Vps34 along with the p-PKCγ (Fig. 1A), suggesting that p-PKCγ and Vps34 are colocalized in the neurons as molecular complex (Fig. 1A). PKC activator PDBu (1 μM for 24 h) significantly increased Vps34 level in MI of the neurons (Fig. 1B).

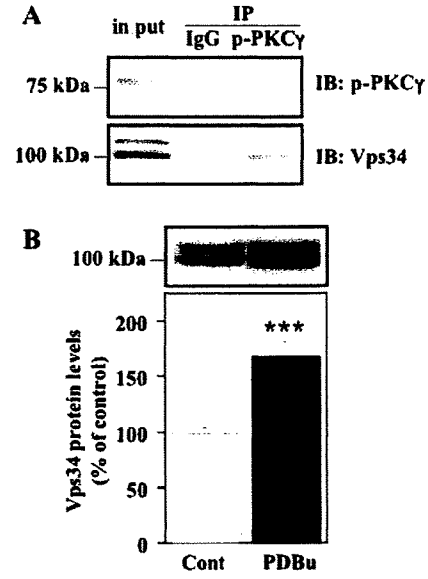

Fig. 1. **A:** Coimmunoprecipitation p-PKCγ and Vps 34 in the cerebrocortical neurons. S1 were immunoprecipitated (IP) with antibody to phospho-PKCγ (p-PKCγ), and then immunoblotted (IB) for p-PKCγ and Vps34. **B:** Vps34-IR in MI. The neurons were exposed to PDBu (1 μM for 24 h). The data represent the mean with SEM ***$P < 0.001$ vs. control (Bonferroni's test; $n = 5$).

As phosphorylation of PKCγ is activated by morphine (Aoki et al., 2004), whether morphine regulates the upregulation of Vps34 was examined. Figure 2A shows that morphine exposure (0.3 μM for 24 h) increases PKCγ phosphorylation in S1 of the neurons. We further investigated whether the increase of PKCγ phosphorylation regulates Vps34 during morphine exposure. Morphine exposure significantly increased Vps34 level, which was significantly suppressed by CHL (1 μM for 24 h), a PKCγ inhibitor, in MI (Fig. 2B).

DISCUSSION

Vps34 forms a heterodimer with Vps15, a serine/threonine kinase (Stack et al., 1993) and localizes in Golgi apparatus and endosomes (Stack and Emr, 1994). Vps34 regulates vesicular trafficking in the endosomal/lysosomal system and participates in the recruitment of proteins with PI(3)P-binding domains to intracellular membranes (Lindmo and Stenmark, 2006). On the other hand, PKCγ works as a serine/threonine kinase to control numerous signaling cascades by phosphorylating target proteins such as neurotransmitter receptors, G proteins, and ion-channels as other kinases do (Hug and Sarre, 1993; Premont et al., 1995). As shown in this study, p-PKCγ and

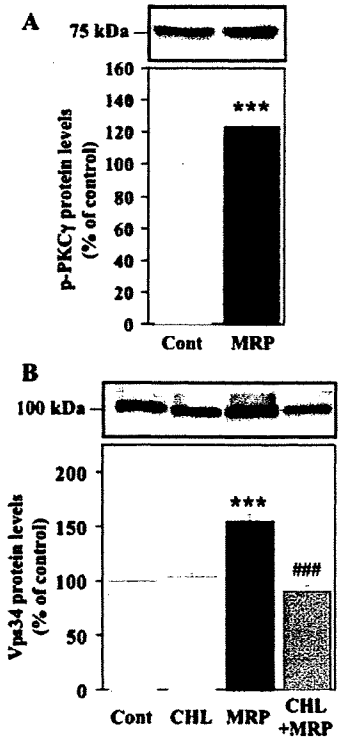

Fig. 2. **A:** Upregulation of p-PKCγ-IR in S1 of the neurons. The neurons were exposed to morphine (MRP; 0.3 μM for 24 h). The data represent the mean with SEM $^{***}P < 0.001$ vs. control (Bonferroni's test; $n = 5$). **B:** Changes in Vps34 level in MI of the neurons during morphine exposure. The neurons were exposed to morphine (MRP; 0.3 μM for 24 h) and/or PKC inhibitor CHL (1 μM for 24 h). The data represent the mean with SEM $^{***}P < 0.001$ vs. control. $^{###}P < 0.001$ vs. MRP (Bonferroni's test; $n = 5$).

Vps34 are present together in molecular complexes in S1 of the neurons and the stimulation of PKC by PDBu upregulates Vps34 in MI of the cortical neurons. These results suggest that Vps34 may be translocated to Golgi and endosomes by activation of PKCγ and produce the PI(3)P for regulation of membrane trafficking.

A recent paper reported the blockade of carbachol-stimulated degranulation by inhibitory antibodies to hVps34 in the cells overexpressing M_1 muscarinic receptors (Windmiller and Backer, 2003), which suggests a link between hVps34 and $G_{\alpha q}$-coupled receptors. In addition, several investigations provide a direct link between trimeric G-proteins and Vps34-Vps15 (Slessareva et al., 2006; Volinia et al., 1995). On the other hand, previous reports have also revealed that a $G_{\alpha q}$-coupled receptor, metabotropic glutamate receptor 5 (mGluR5), relates to the development of morphine-induced rewarding effect (Aoki et al., 2004) and that upregulation of the $G_{\alpha q/11}$ protein and PKC is important in the development of sensitization to morphine-induced hyperlocomotion (Narita et al., 2002). Several lines of evidence suggest that glutamatergic projections to the nucleus accumbens originating from prefrontal cortex, hippocampus and amygdala (Meredith et al., 1993) regulate emotional and behavioral processing. Therefore, it is suggested that activation of glutamatergic neurons by morphine causes regulation of Vps34 through the stimulation of mGluR5, $G_{\alpha q/11}$, and PKCγ cascade in the nucleus accumbens. In fact, this study demonstrates that morphine increases both Vps34 and p-PKCγ protein levels and inhibition of PKCγ suppresses the upregulation of Vps34. Thus, it is speculated that upregulation of Vps34 by morphine in the Golgi apparatus and endosomes facilitates, in turn, the trafficking of several protein serving in vesicular transport or recycling systems. These findings provide direct evidence that upregulation of Vps34 is mediated through the activation of PKCγ during morphine treatment.

In conclusion, these data indicate that p-PKCγ and Vps34 are present together in molecular complexes in the neurons. The treatment with morphine increases PKCγ and Vps34 levels. The inhibition of morphine-induced increase in PKCγ phosphorylation reduced Vps34 level. These results indicate that opioid receptor activation increases PKCγ phosphorylation in the neurons and, in turn, upregulates Vps34 during short-term treatment with morphine.

ACKNOWLEDGMENTS

The authors thank Noriko Ohtsuki and Junko Katayama for their excellent technical assistance.

REFERENCES

Aoki T, Narita M, Shibasaki M, Suzuki T. 2004. Metabotropic glutamate receptor 5 localized in the limbic forebrain is critical for the development of morphine-induced rewarding effect in mice. Eur J Neurosci 20:1633–1638.

De Matteis MA, Godi A. 2004. PI-loting membrane traffic. Nat Cell Biol 6:487–492.

Futter CE, Collinson LM, Backer JM, Hopkins CR. 2001. Human VPS34 is required for internal vesicle formation within multivesicular endosomes. J Cell Biol 155:1251–1264.

Hug H, Sarre TF. 1993. Protein kinase C isoenzymes: divergence in signal transduction. Biochem J 291:329–343.

Herman PK, Stack JH, Emr SD. 1992. An essential role for a protein and lipid kinase complex in secretory protein sorting. Trends Cell Biol 2:363–368.

Kose A, Saito N, Ito H, Kikkawa U, Nishizuka Y, Tanaka C. 1988. Electron microscopic localization of type I protein kinase C in rat Purkinje cells. J Neurosci 8:4262–4268.

Kose A, Ito A, Saito N, Tanaka C. 1990. Electron microscopic localization of γ- and βII-subspecies of protein kinase C in rat hippocampus. Brain Res 518:209–217.

Lindmo K, Stenmark H. 2006. Regulation of membrane traffic by phosphoinositide 3-kinases. J Cell Sci 119:605–614.

Lowry OH, Rosebrough NJ, Farr AL, Randall RJ. 1951. Protein measurement with the Folin phenol reagent. J Biol Chem 193: 265–275.

Meredith GE, Pennartz CM, Groenewegen HJ. 1993. The cellular framework for chemical signaling in the nucleus accumbens. Prog Brain Res 99:3–24.

Narita M, Mizuo K, Shibasaki M, Narita M, Suzuki T. 2002. Up-regulation of the $G_{q/11\alpha}$ protein and protein kinase C during the development of sensitization to morphine-induced hyperlocomotion. Neuroscience 111:127–132.

Noble F, Szücs M, Kieffer B, Roques BP. 2000. Overexpression of dynamin is induced by chronic stimulation of μ- but not δ-opioid receptors: relationships with μ-related morphine dependence. Mol Pharmacol 58:159–166.

Ohkuma S, Tomono S, Tanaka Y, Kuriyama K, Mukainaka T. 1986. Development of taurine biosynthesizing system in cerebral cortical neurons in primary culture. Int J Dev Neurosci 4:383–395.

Premont RT, Inglese J, Lefkowitz RJ. 1995. Protein kinases that phosphorylate activated G protein-coupled receptors. FASEB J 9:175–182.

Slessareva JE, Routt SM, Temple B, Bankaitis VA, Dohlman HG. 2006. Activation of the phosphatidylinositol 3-kinase Vps34 by a G protein α subunit at the endosome. Cell 126:191–203.

Stack JH, Herman PK, Schu PV, Emr SD. 1993. A membrane-associated complex containing the Vps15 protein kinase and the Vps34 PI 3-kinase is essential for protein sorting to the yeast lysosome-like vacuole. EMBO J 12:2195–2204.

Stack JH, Emr SD. 1994. Vps34p required for yeast vacuolar protein sorting is a multiple specificity kinase that exhibits both protein kinase and phosphatidylinositol-specific PI 3-kinase activities. J Biol Chem 269:31552–31562.

Volinia S, Dhand R, Vanhaesebroeck B, MacDougall LK, Stein R, Zvelebil MJ, Domin J, Panaretou C, Waterfield MD. 1995. A human phosphatidylinositol 3-kinase complex related to the yeast Vps34p-Vps15p protein sorting system. EMBO J 14:3339–3348.

Windmiller DA, Backer JM. 2003. Distinct phosphoinositide 3-kinases mediate mast cell degranulation in response to G-protein-coupled versus FcepsilonRI receptors. J Biol Chem 278:11874–11878.

Zhang Y, Helm JS, Senatore A, Spafford JD, Kaczmarek LK, Jonas EA. 2008. PKC-induced intracellular trafficking of Ca_V2 precedes its rapid recruitment to the plasma membrane. J Neurosci 28: 2601–2612.